SMN depletion has a differential effect on expression of *Igf1* and *Trp53* in the CNS and peripheral tissues of two different mouse models of Spinal Muscular Atrophy

Morgan Donoghue

This thesis is submitted in partial fulfillment of the requirements for the Master of Science degree in Cellular and Molecular Medicine

Department of Cellular and Molecular Medicine

Faculty of Medicine

University of Ottawa

Supervisor: Dr. Rashmi Kothary

Table of Contents

Abstract

Spinal Muscular Atrophy (SMA) is a debilitating neurodegenerative disease resulting in death of the lower motor neurons, muscle atrophy, and in severe cases death. Due to mutations or deletions in the Survival Motor Neuron 1 (*SMN1*) gene, levels of functional SMN protein product are decreased. While SMA was previously described as a motor neuron exclusive disorder, recent evidence suggests that many tissue and cell types throughout the body are affected. The objective of our study was to outline the effects of varying levels of SMN depletion on two genes of interest, namely Insulin-like growth factor 1 (*Igf-1*) and Tumor suppressor protein 53 (*Trp53*) in multiple tissues throughout disease course. The severe $Smn^{2B/-}$ and mild $Smn^{2B/-}$; $SMN2^{+/-}$ mouse models of SMA were utilized in our studies to determine the levels of mRNA expression and subsequent protein output for these two genes. We employed RT-qPCR, western blot, and ELISA experimental methods. In $Smn^{2B/-}$ mice, *Igf-1* mRNA was substantially decreased in symptomatic liver tissue. This was accompanied by widespread decrease in IGF-1 protein in peripheral tissues. Interestingly, this depletion effect on *Igf-1* was not observed in the mild mouse model. Our analysis also showed that *Trp53* mRNA was dramatically increased within tibialis anterior skeletal muscle of symptomatic $Smn^{2B/-}$ mice, alongside an upregulation of factors involved in p53 mediated apoptosis. Once again, this effect was not observed in the mild $Smn^{2B/-}$; $SMN2^{+/-}$ mouse model. Overall, we have demonstrated that the extent of SMN depletion, determines whether the expression of *Igf-1* and *Trp53* is perturbed, suggesting that disease severity is an important factor in what pathways are affected. Finally, we show that alterations in gene expression patterns or subsequent protein levels act in a tissue-specific fashion. More investigation is encouraged to highlight IGF-1's role as a potential SMN-independent therapeutic for SMA.

Acknowledgments

I would like to acknowledge and thank my wonderful friends and colleagues in the Kothary laboratory for their patience, support, and guidance throughout the process of my MSc program. Lucia, Kelsey, and Aoife displayed such passion and understanding in their experimental teachings while Dr. Kothary and Dr. Hansel provided valuable knowledge and advice when I hit roadblocks. Additionally, my work could not have been completed without the technical support of Rebecca, Ariane, Sabrina, and Yves to which I'm incredibly grateful.

I would also like to thank my sister Madison and partner Ryan who were always there to give advice, relax with, and listen to my unsolicited science rants. Their unconditional love and support truly mean the world to me.

Finally, I wish to acknowledge and dedicate my MSc thesis to my brother Mitchell. You made me laugh in moments of heartbreak, smile in moments of frustration, and party when there was due cause for celebration. While you were not personally a fan of higher education, you never wavered in your support because I am a "giant nerd". I will miss you forever Mitchell. Until we meet again.

List of Figures

List of Abbreviations

AAV9 – adeno-associated virus 9

ActB – beta actin

Akt – protein kinase B

ASO – antisense oligonucleotide

Bad – Bcl-2-associated death promotor

Bax – Bcl-2 associated X protein

Bbc3 – Bcl-2 binding component 3

BCA assay – Bicinchoninic Acid protein assay

Bcl2 – B cell leukemia/lymphoma 2

CB – coiled bodies

Cdkn1a – cyclin-dependent kinase inhibitor 1

cDNA – complementary DNA

CNS – central nervous system

DNA – deoxyribonucleic acid

ECG – electrocardiogram

ECL – enhanced chemiluminescence

ELISA – enzyme linked immunosorbent assay

FL-SMN – full length survival motor neuron

Igf-1 – insulin-like growth factor 1

IGF-1R – insulin like growth factor 1 receptor

Igfals – Insulin-like growth factor binding protein, acid labile subunit

IGFBP – Igf-1 binding protein

ISS-N1 – intronic splicing silencer N1

IVS – interventricular septum

LV – left ventricle

Mdm2 – Mouse double minute 2

MHC – myosin heavy chain

miRNA – micro-RNA

MN – motor neuron

MOM – mitochondrial outer membrane

mRNA – messenger RNA

mTOR – mammalian target of rapamycin

NAFLD – non-alcoholic fatty liver disease

NMD – nonsense mediated decay

NMJ – neuromuscular junction

P21 – cyclin-dependent kinase inhibitor 1 (protein 21)

P53 – tumor protein 53

Pmaip1 – phorbol-12-myristate-13-acetate-induced protein 1

P-P53 – phosphorylated tumor protein 53

Pre-mRNA – pre messenger RNA

RNA – ribonucleic acid

RT-qPCR – real time quantitative PCR

SC – spinal cord

SMA – spinal muscular atrophy

SMN – survival motor neuron

SMN1 – survival motor neuron 1

SMN2 – survival motor neuron 2

sno-RNP – small nucleolar ribonucleoprotein

snRNA – small nuclear RNA

snRNP – small nuclear ribonucleoprotein

TA – tibialis anterior

Trp53 – tumor suppressor protein 53

WB – western blot

1. Introduction

1.1 Spinal Muscular Atrophy

Spinal muscular Atrophy (SMA) is a devastating neurodegenerative condition characterized by the death of alpha motor neurons (MNs).[1] Following MN death, symptoms can range from generalized muscle weakness, mobility impairments, respiratory complications, and cardiac deficits depending on the severity of disease.[1]

Prevalence and Etiology

SMA is the leading genetic cause of infant mortality with a prevalence of 1:10000 live births.[1] Due to the mutation or deletion of the survival motor neuron 1 (*SMN1*) gene,[1] reliance on a near identical gene, survival motor neuron 2 (*SMN2*) is required. *SMN2* however produces a truncated and unstable survival motor neuron (SMN) protein product. A single nucleotide transition within the exon 7 region of *SMN2* results in alternative splicing and predominant production of this non-functional product which excludes exon 7.[1] Only approximately 10% of *SMN2* protein product is full length and stable. It is for this reason that the number of *SMN2* gene copies available mediates disease severity by increasing the levels of full length SMN (FL-SMN) available. The more functional SMN bioavailable, the less severe the disease manifests.

Classification

The degree of SMA disease severity is dependent on the number of available *SMN2* gene copies. Increased copies of *SMN2* results in the production of more functional SMN protein

which leads to a milder form of SMA.[2] It is due to this range of *SMN2* allele copies that SMA is classified into four subgroups ranging from type 0 – type 4.[2]

A type 0 SMA diagnosis typically refers to neonates that present with decreased fetal movement, hypotonia and generalized weakness. With only one copy of *SMN2*, very little functional SMN is produced and life expectancy is typically less than 6 months of age.[2]

Type 1 SMA, also referred to as Werdnig-Hoffman disease, also presents with generalized weakness, hypotonia, and poor reflexes. These individuals miss major motor milestones including the ability of sitting upright unassisted and walking. Type 1 SMA patients typically have 2-3 copies of the *SMN2* gene, and a life expectancy of 2 years.[2]

Type 2 SMA patients in contrast to type 1, will gain the ability to sit unassisted throughout life. Hypotonia, proximal muscle weakness, and the loss of walking milestone are common in this group.[2] In addition to this, orthopedic abnormalities begin to present including scoliosis of the spine. On average, these patients will possess approximately 3 copies of the *SMN2* gene and have a diagnosis between 3-15 months of age.[3]

Type 3 SMA begins the threshold of mild disease onset of SMA. These individuals will present with 3-4 copies of *SMN2* and the ability of sit and crawl unassisted. Some patients will reach the walking milestone, although they will still present with proximal muscle weakness of the legs specifically. A full life expectancy is expected for this group.[2]

Finally, type 4 SMA is considered a rare adult-onset form of the disease. Similar to type 3 patients, this group will reach motor milestones and begin to develop symptoms, such as muscle weakness, after the age of 30.[2] These individuals possess 4+ copies of the *SMN2* gene which delays onset of the condition. A full life expectancy is also anticipated for these patients.

1.2 Structure and Functionality of SMN

Survival Motor Neuron is a protein which has a variety of essential housekeeping roles within the cell. Primarily, SMN is involved in pre-mRNA splicing, RNA metabolism, DNA repair, and intracellular trafficking.[4] However, alternative splicing of the *SMN1* and *SMN2* genes may result in protein products which alter these abilities. To begin, once must understand the structure and components of *SMN1*, *SMN2*, and the various SMN protein isoforms to highlight their roles in cellular development and housekeeping.

SMN1 and *SMN2* Gene Structure and Alternative Splicing

SMN1 and *SMN2* are located on telomeric and centromeric regions of chromosome 5q13 respectively.[5] It is due to the process of duplication and inversion of this 500 kb region which allows *SMN2* to exist in humans. As such, *SMN1* and *SMN2* share more than 99% nucleotide identity.[5] Each 1.5 kb transcript of these genes are then capable of producing SMN protein products. However, due to a point mutation within exon 7, the splicing activator is unable to bind causing *SMN2* to primarily produce transcripts and subsequent protein product which excludes the exon 7 region (SMNΔ7).[4]

Other transcripts produced by the *SMN1* and *SMN2* genes have also been identified including α-SMN and SMN6B transcripts. Unfortunately, the overall functionality and stability of these transcripts are incompletely understood. Some evidence suggests that α-SMN, a transcript isoform resulting by the retention of intron 3, produces a product which aids in axonal development and growth, stimulates cell motility, and regulates chemokines.[6] This isoform is only observed in early stages of development as it becomes degraded through the nonsense mediated decay (NMD) pathway.[4,6] Concurrently, the detection of transcript isoform SMN6B is

also incompletely characterized. SMN6B, created by the inclusion of an Alu-like sequence within intron 6, is also eliminated by NMD but remains more stable than the SMNΔ7 isoform.[7] Altogether *SMN1* and *SMN2* can produce alternatively spliced transcript isoforms, however more investigation is required to highlight their function, stability, and translation into protein product.

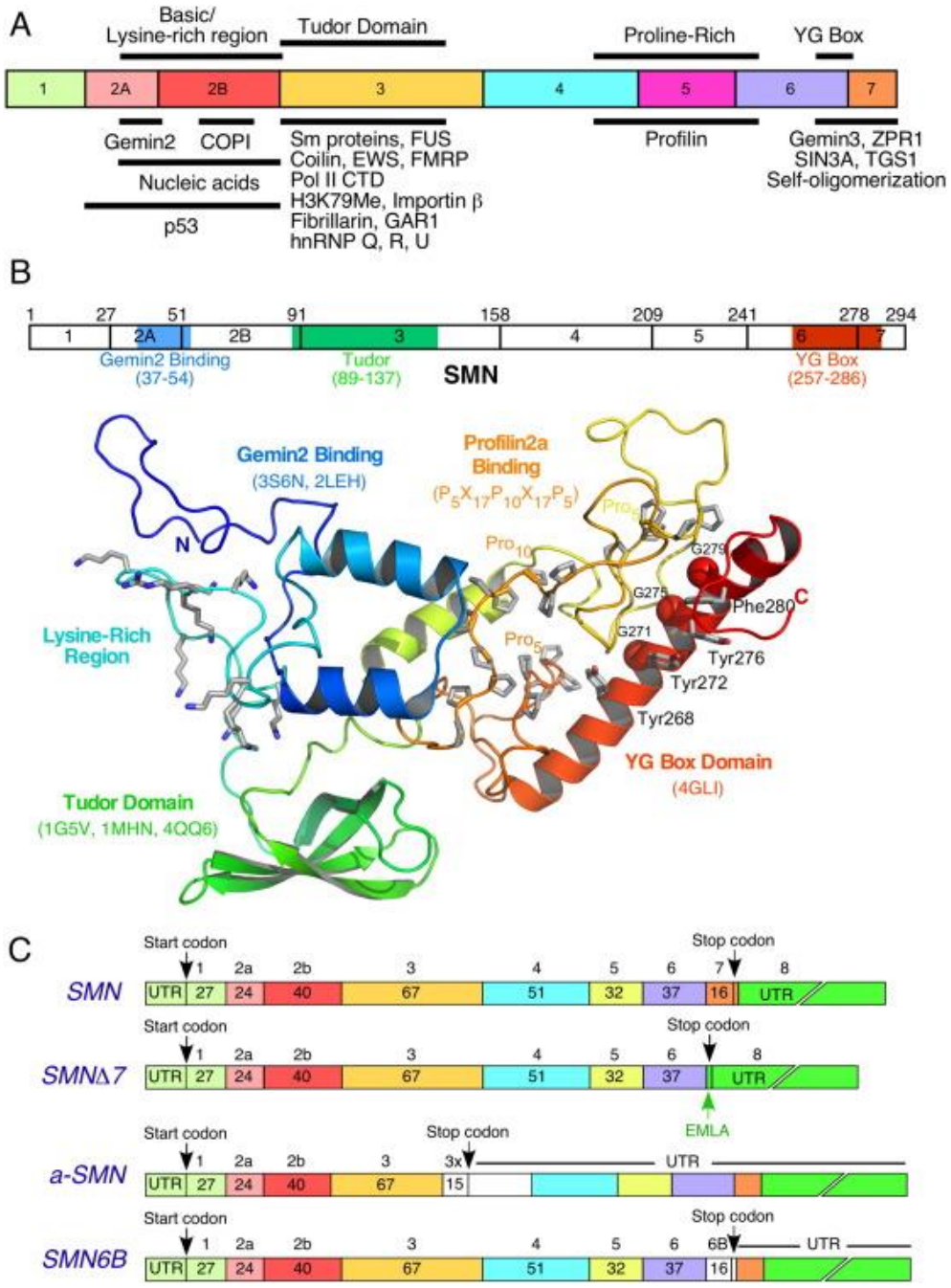

Figure 1. Protein domains and interacting partners of SMN protein alongside identified *SMN1* and *SMN2* transcript isoforms. A) Protein domains of SMN categorized by corresponding exon region. Interacting partners are listed under corresponding domain title. B) Three dimensional SMN protein structure colourized by domain. C) Identified *SMN*1 and *SMN2* transcript isoforms. Isoform name is listed to the left of transcript diagram, colour coded by exon region. Image acquired by (Singh *et al*., 2017).[4]

SMN Protein Domain Organization and Interacting Partners

FL-SMN protein is a 38 kDa protein organized into four domains spanning its 294 amino acids. Each domain possesses the ability to interact with select protein partners to complete its cellular housekeeping roles.

The first N-terminal domain consists of a lysine rich region responsible for binding with SMN interacting protein 1 (SIP1) also known as Gemin 2. It is the SMN-Gemin 2 complex which is central to SMN's role in facilitation snRNP biogenesis, signal recognition particle biogenesis, DNA recombination, and translation regulation. This protein region also directly interacts with p53, another transcription regulator known for its role in apoptosis.

Secondly, the central Tudor domain has been characterized to interact with proteins containing RGG/RG motifs. These include GAR1, hnRNP Q, hnRNP R, hnRNP U, Sm proteins, Histone 3 and the carboxy terminal domain (CTD) of RNA Polymerase II (pol II). Altogether these interaction work to regulate transcription, and translation of mRNAs within stress granules of the cell.

Downstream of the central Tudor domain is a proline rich region associated with the interaction of profilins. Together, SMN-Profilin interactions work to stabilize actin dynamics such as the homeostasis of the actin cytoskeleton. Interestingly, SMN mutations are associated with the splicing defects of the Profilins gene and subsequent impaired actin dynamics.[8]

Finally, the final C terminal domain spanning exons 6 and 7 include a YG box and sequence involved in self-oligomerization. Specifically, this domain elicits an important role in its overall stabilization and localization within the cell.

Overall, the relationship between SMN protein domains and their respective interacting partners are crucial in maintaining SMNs ability to complete its functions in RNA metabolism, transcription regulation, splicing, and self-stability.

1.3 Role of SMN protein in the CNS and periphery

Through its interacting partners such as Sm proteins, Gemin 2/SIP1, p53, profilins and RNA polymerase III, SMN protein is capable of preforming diverse functions within the cell. In situations of depleted SMN, interaction with partners to complete roles are unsuccessful. As such, models of SMA have been developed to investigate how low levels of SMN influence the molecular landscape of SMA.

Models of SMA

When developing models to investigate SMA, it is important to replicate the systemic effects SMN depletion has on the body, which is comparable and translatable to the human SMA population. To achieve this, many researchers utilize mouse models developed to express low levels of SMN protein throughout all the cell types. Here we will discuss the main current models used in SMA research.

Cell Line Models of SMA

While SMA has recently been recharacterized as a multi-system condition, it is not uncommon to see the use of various cell models subjected to SMN depletion through various methods. One of the main benefits of these models are to isolate the given tissue/cell type from

other organs/systems that may influence or mask an effect. For example, using a skeletal muscle cell line, C2C12, to observe the innate defects that SMN depletion has on skeletal muscle removes the influence of neuromuscular junction (NMJ) and MN loss. While this is a benefit it can also be a limitation to a study. We know in SMA patients, skeletal muscle cells do not act in isolation, but rather as a part of a system. Therefore, current studies often compare cell line data to results from more holistic models such as mouse models.

Mouse Models of SMA

Throughout the last two decades of research being conducted in the field of SMA, many different mouse models have been developed to begin to highlight the holistic effects that SMN depletion has throughout the body. To allow them to still be translatable to the patient population, various methods are employed to reproduce the SMN protein depletion (rather than complete absence).

The models that represent the more severe forms of SMA include the Taiwanese, SMNΔ7, and *Smn*$^{2B/-}$ models of SMA. The most severe model, labeled the Taiwanese model, is generated by introducing a human *SMN2* transgene to an *Smn*$^{-/-}$ mouse. This was done by crossing two *Smn*$^{+/-}$*;SMN2* mice, as a full Smn knockout mouse is embryonically lethal.[9] Taiwanese mice display progressive muscle loss and atrophy, motor impairments, hindlimb paralysis and premature death as early as P10.[9] In a similar fashion, the SMNΔ7 model also displays a severe phenotype of MN loss, muscle atrophy and death by P14. SMNΔ7 mice however contain both an *SMN2* and *SMNΔ7* transgene, which compared to the Taiwanese model extends lifespan and some pathologies minimally.[10] Finally, a less severe model of SMA commonly utilized in the literature is the *Smn*$^{2B/-}$ model. By mutating the exonic enhancer region of the mouse *Smn* gene at exon 7, one can generate a murine *Smn* gene which behaves more like

the human *SMN2* gene.[11] The mutation in the mouse *Smn* gene was called the 2B mutation, and in conjunction with a *Smn* null allele, produces mice which experience MN loss, motor defects, reduced body weight and NMJ pathologies. These mice can survive up to P28 depending on genetic background.[11] Interestingly, this model displays no overt symptoms until P10 which provides the opportunity to better understand defects as they progress across disease course.[11]

It is important to note that much research has been conducted to investigate the molecular landscape of the most severe forms of SMA. Unfortunately, more work is needed to compare these findings to more mild forms of the disease. The $Smn^{2B/-}$; $SMN2^{+/-}$ mouse model achieves just this. By introducing one *SMN2* transgene to the $Smn^{2B/-}$ background, a mild phenotype of SMA is generated.[12] Mild motor defects, denervation, and NMJ pathology was observed, however mice experienced normal survival and a general lack of extra-neuronal pathologies.[12]

Given these four predominant models of SMA in current research, investigators can begin to understand SMA pathology throughout various levels of SMN depletion and stages of life. There is a dire need to understand specifically the similarities and differences of SMN downstream molecular changes between different severities of SMA. They offer an important holistic approach to testing novel therapeutics as well as understanding pathways of disease progression at the cellular level.

Patient / Clinical Models of SMA

Finally, patient / clinical data also provide excellent sources of information when investigating SMA therapies, comorbidities, and pathways of disease at the cellular level. From using donated patient tissue samples, patient derived cell lines, and epidemiological data, one can study outcomes utilizing the most transferable method. However, one drawback which must be

acknowledged is understanding and respecting treatment first ethics. Interventions for instance must be restricted to those which are predicted to have a positive effect and to cause the least amount of harm possible. In addition, finding ethically available control groups within the patient population pose moral dilemmas. Clinical trials for therapies undergo extensive and expensive study in multiple other model types before reaching the bedside.

In conclusion, many model types including cell, mouse, and patient models are all commonly used throughout the field of SMA research. While each model provides separate limitations and benefits, it is critical that the appropriate model or models are used to answer the specific hypothesis in question.

SMN and the Spliceosome

Additional complications of SMN deficiencies observed in SMA may be attributed to SMN's role in pre-mRNA splicing and the maturation of splicing machinery. Splicing roles are not limited to only neuronal tissue; therefore, these impairments may transcend several different cell types. To first address this issue, one must understand the spliceosome as well as the role SMN plays in snRNP biogenesis and the processing of pre-mRNA.

The spliceosome is a complicated macromolecule involved in the removal of introns from pre-mRNA transcripts. With the use of small nuclear ribonucleoproteins (snRNPs) within the nucleus, a complex is developed which "snips" the non-coding regions of the pre-mRNA called introns, and connects the coding regions, called exons, into the final mRNA transcript ready to be exported from the nucleus to the cytosol to undergo translation. It is at the level of snRNP biogenesis and transportation that SMN protein contributes to the spliceosome.

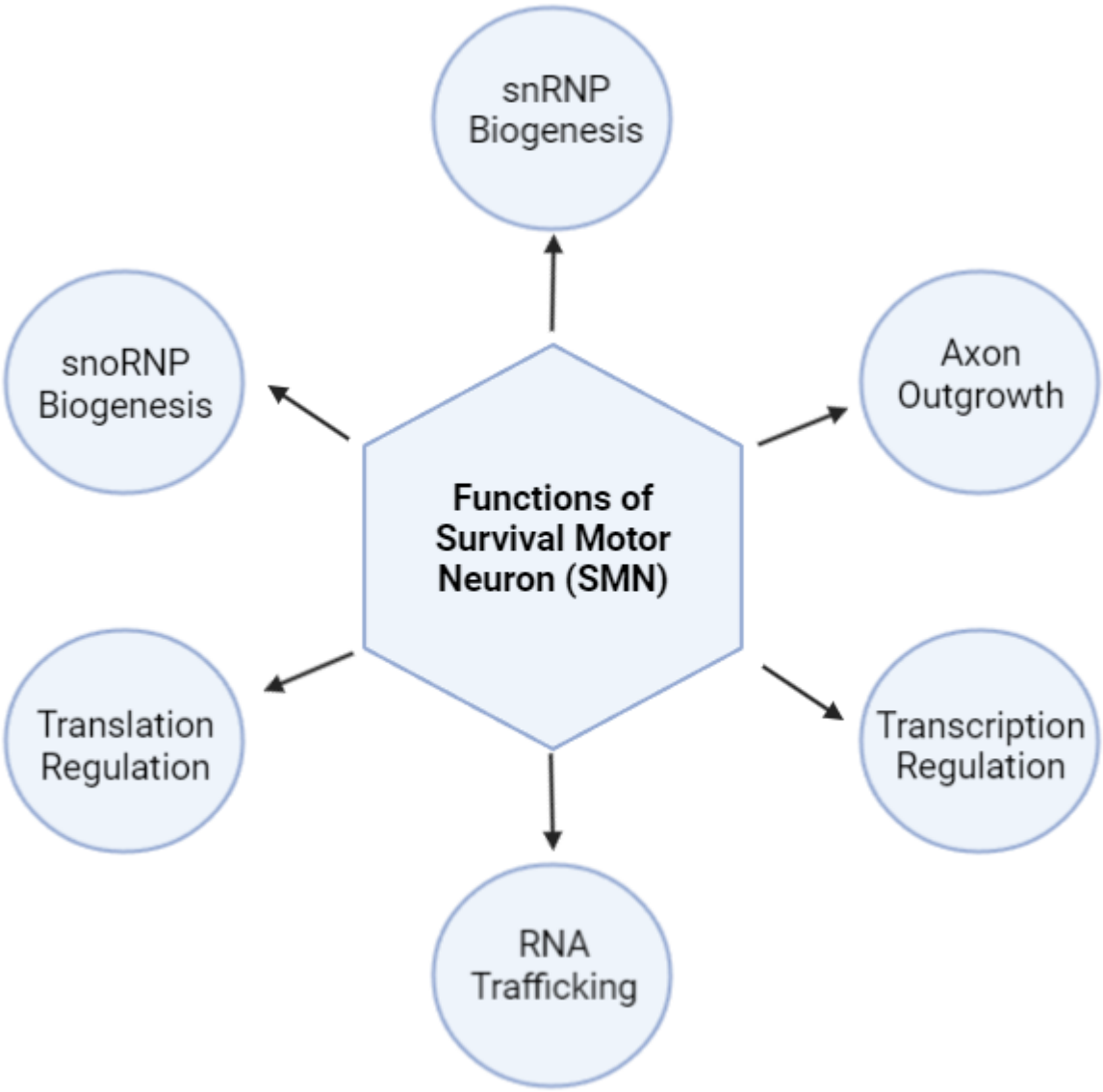

Figure 2. Summary of SMN functions within the cell. SMN plays various roles in RNA metabolism and development. Being ubiquitously expressed, SMN is in nearly every cell type in the body and is critical for development. Created by BioRender.

Within the cell, SMN is ubiquitously expressed in both nuclear and cytosolic compartments.[4,13] It is in the nuclear compartment however that we observe SMN's first role of creating nuclear gems, which share many characteristics with Cajal (coiled) bodies.[4,13] These regions of the nucleus act as a snRNP maturation site and houses snRNAs. In addition to this

however it is observed that SMN protein also plays a critical role in the formation of an SMN complex within the cytosol. This cytosolic SMN complex, composed of SMN, Gemin 2-8, Unrip, and Sm proteins, then acts to chaperone the translation of snRNA to snRNPs.[4,13] After the biogenesis of snRNPs, SMN also aids in the binding of its signal recognition particle (via WRAP53) to return the finished snRNP back to the nucleus to perform its function in the spliceosome.[13] Given these multiple functions SMN acquires in snRNP biogenesis as well as RNA metabolism, it is perhaps unsurprising that SMN depletion hosts a range of devastating effects in this area.

Overall, it is well documented that SMN protein has many functions in the creation of the spliceosome and RNA metabolism in general. Given how this biological process occurs in every cell type, it is important to investigate the effects of SMN depletion in a range of tissues.

SMN and Development

SMN protein plays a vital role in the development of tissues at both embryonic and neonatal stages of life in mammals. Interestingly, the level of SMN in select regions of the developing body varies depending on time and tissue type. For example, highest expression of SMN protein are observed in the CNS of young mice.[14] This increase in protein aids in the outgrowth of axons in the CNS, subsequent muscle growth, and stimulates cell motility. SMN is so crucial in fact, that complete SMN knock-out models are embryonically lethal.

Over time into adulthood, SMN levels naturally decline into lower baseline concentrations. For example, one study investigated the role of SMN protein in adult SMNΔ7 mice in various tissue types. By utilizing an *SMN2* mRNA splicing modulator treatment, analogous to risdiplam, the severe SMNΔ7 mice were dosed from neonates (P3) until P40 when

treatment was then withheld. It was found that SMN protein returned to low baseline levels after the withdrawal of treatment, followed by progressive muscle atrophy, weight loss, and necrosis (P75).[15] Interestingly, mice who experienced withdrawal did not exhibit loss of NMJs or muscle innervation. These findings were then compared to SMNΔ7 mice that were continuously dosed, which displayed a generalized lack of pathology. Overall, it was concluded that SMN protein remains necessary throughout the full lifespan of this mouse model, with particular interest of tissues beyond the MN and NMJ such as muscle.[15]

It is well documented that SMN is fundamental in the development and maintenance of ranges of tissues throughout the lifespan. While emphasis is placed on SMN's role in the neonatal CNS, more investigation is required to understand SMN's role at the molecular level, throughout life, and in multiple tissue types.

SMN Roles and Pathologies in Varying Tissue Types

Given the critical function of SMN protein in development of tissues and RNA metabolism, it is important to highlight the role and interacting partners of SMN in varying tissue types. Between the variation in SMN interacting partners and SMN isoform type, SMN depletion may have differential effects in different organs.

Central Nervous System

Due to alternative splicing, up to eight potential isoforms of SMN protein are produced in humans between the *SMN1* and *SMN2* genes. These isoforms have been identified as playing a role in cell motility, axon growth, and stimulation of C-C Motif Ligand 2 (CCL2), and Insulin-like Growth Factor-1 (IGF-1) production.[6] As the name suggests, SMN plays an integral role in the survival and development of motor neurons specifically.

This function can be further highlighted by studies which investigate SMN localization in cell models throughout development. In one such study, it was observed that in rat brain and embryonic chick neurite cell lines, FL-SMN was distributed ubiquitously throughout the cell, in granules which resided in growth cones and neurites.[16] When cells were introduced to SMN lacking exon 7, SMN failed to localize into the cytoplasm and ultimately resulted in stunted neurite growth.[16] Interestingly, more evidence supports this conclusion using knock down models. Using primary cultures of hippocampal cells in which full length-SMN was selectively silenced, it was observed that neurites lost neuronal polarity as well as reduced axon growth.[17] At the cellular level it has been well documented that SMN is critical in the maturation of neuronal cell types.

At a more macroscopic level, it is also observed that *smn1* gene silencing in MNs of zebrafish models results in the hallmark characteristics of SMA.[18] For example, this study generated an anti-*smn1* microRNA (miRNA) to selectively decrease SMN levels in given tissues and timepoints.[18] This anti-*smn1* miRNA elicits post-transcriptional control of the *smn1* gene by binding to and silencing *smn1* mRNA in the zebrafish model. When anti-*smn1* miRNA expression was only expressed within motor neurons, and no other tissue, zebrafish experienced MN loss, weight loss and early death.[18] When anti-*smn1* miRNA was then independently expressed in muscle tissue, gross symptomology (weight loss, scoliosis, muscle atrophy) also occurred however only at late timepoints.[18] This provided evidence overall that the loss of MNs specifically due to SMN depletion contributed highly to the hallmark symptoms observed in SMA.

Given SMN's vital role in the development and maintenance of the CNS, and the following consequences of SMN depletion on these tissues, it is perhaps unsurprising that for

many years SMA was thought to be a MN-specific disease. However, when SMN treatments are solely directed to the motor neuron, SMA pathology still persists.[19] Due to this, more recent studies have highlighted the role of SMN in additional tissues independent of the MN.

Heart

SMN's role within cardiac tissue remains under characterized in the literature. However, cardiac defects and abnormalities are often reported in both animal models and SMA patients.

Within the human population, SMN deficiency is inversely correlated with SMA disease severity. The most severe type (Type I), which possess the lowest levels of SMN protein, were most strongly associated with overt cardiac structural abnormalities and obstructions to cardiac outflow whereas mild subtypes were associated with cardiac rhythm disorders.[20] Similarly, electrocardiogram (ECG) deficits such as bradycardia were observed in patients with Type I-III SMA, however Type I patients were more likely to experience these comorbidities.[20] On a microscopic level, histological staining from patient biopsy of cardiac tissue revealed myocardial fibrosis, as well as atrophic and degenerated myocytes within patient samples.[20] Given these symptoms, the question became whether cardiac defects were due to a developmental delay or overt cardiac pathology.

To examine this concept in more detail, mouse models of SMA were utilized to determine the degree of cardiac pathology present throughout the lifespan of SMA affected mice. At the embryonic stages, SMA effected mice of the Taiwanese mouse model were found to have decreased overall heart size at the E14.5 stage of development, but no overt structural abnormalities.[21] By E17.5, another study highlighted interventricular septum (IVS) wall and left ventricle (LV) wall thinning in the same mouse model.[22] Postnatally, cardiac fibrosis was

observed throughout heart cross-sections brought on by oxidative stress. This provided further support for subsequent bradycardia measured in these symptomatic mice.[22]

In general, evidence suggests that there remains under characterized cardiac defects in both human and mouse models of SMA. This furthers our need to generate therapies for and investigate the molecular landscape of non-neuromuscular tissue types in SMA.

Liver

In addition to the overt CNS deficits and cardiac symptomology observed in SMA, pathology is also observed within liver tissue of both patient and mouse models of the disease. From altered liver function and perturbations in iron homeostasis, to gross pathology such as dyslipidemia and non-alcoholic fatty liver disease (NAFLD), liver deficits outline another MN independent disease aspect of SMA.

From a developmental perspective, it has been observed that SMN protein is required for the successful development of a functional organ. Strikingly, when SMA livers within the Taiwanese mouse model were compared to littermate controls at E14.5, substantial changes were observed within the liver proteome.[21] While total volume size of these embryonic livers remained unchanged, it was found that many proteins within embryonic development pathways were highly dysregulated.[21] Utilizing the same mouse line postnatally, it was established that these embryonic defects continued to participate in liver dysfunction throughout the lifespan.[23] The observed deficits included defective iron homeostasis, unorganized sinusoids, increased liver platelet production and clotting.[23] It was concluded that there was gross liver developmental failure. Interestingly, when SMA affected mice were systematically given an SMN increasing treatment (ASO), all liver pathologies were ameliorated by a late symptomatic timepoint.[23]

Another fascinating finding within SMA affected mouse livers is the presence of non-alcoholic fatty liver disease (NAFLD). Specifically, the *Smn*$^{2B/-}$ model of severe SMA in recent years has been used to investigate NAFLD due to its good representation of the condition. In a study that examined these livers, it was ultimately concluded that an accumulation of non-esterified fatty acids participated in the creation of reactive oxygen species by mitochondria.[24] These reactive oxygen species then resulted in overall hepatic dysfunction as well as perturbations in protein output. In addition, *Smn*$^{2B/-}$ livers also developed microvesicular steatohepatitis as well as displayed the molecular markers of fibrogenesis.[24] This evidence was further supported by an additional study which observed dyslipidemia, abnormal fatty acid metabolism, and increased hepatic triglycerides in the same mouse model.[25] When they compared these findings to collected patient data, it was uncovered that SMA patients were also susceptible to developing dyslipidemia, liver steatosis, and fatty liver disease.[25]

Given this evidence of developmental and functional defects within liver tissues of both mouse and humans, the role of SMN protein in fatty acid metabolism, liver development, and SMA disease progression requires further investigation. In addition, these liver defects highlight a MN independent pathology component of SMN.

Muscle

Finally, recent developments have begun to outline muscle intrinsic pathologies due to SMN depletion which occur prior to MN death and subsequent muscle denervation. Several recent investigations have described an independent task that SMN protein undertakes in the development and maintenance of muscle tissues. Specifically, SMN's contribution to skeletal muscle cell maturation, differentiation, and proliferation have been highlighted in both cell lines and mouse models of SMA.

Cell lines, for example, provide an excellent model to investigate the isolated effects of SMN depletion on one given tissue type. Importantly, this method can outline muscle defects without the masking effects of corresponding NMJ denervation and MN loss. In the mouse myoblast cell line C2C12 for instance, subjection to SMN knockdown (via siRNA) resulted in earlier expression of myosin heavy chain (MHC), which suggested a faster differentiation process into myotubes or muscle fibers.[26] In conjunction with this however, it was found that the average number of nuclei within these developing myotubes were reduced in the SMN knockdown cells. Given this, it was concluded that SMN depleted C2C12 cells experienced impaired maturation in general.[26] To affirm these findings, mouse models with selective SMN knockdown to skeletal muscles were generated for comparison.

A fascinating study for example utilized a Cre-LoxP system to selectively reduce the level of functional Smn protein only within the skeletal muscle.[27] From there, mice were then bred to express either 1 or 2 copies of the *SMN2* gene systemically. In muscle-specific knock down mice it was observed that muscle defects were present in the absence of MN death. Muscle fibre size decreased, motor impairments became present, and mice overall experienced premature death. Strikingly, when SMN therapies were introduced to these mice at the beginning of symptom onset, the muscle deficits were corrected.[27]

In conclusion, SMN depletion has been observed to participate in pathogenic phenotypes observed in various tissues. While the damage to the CNS is devastating, evidence such as cardiac abnormalities, NAFLD, and MN independent muscle atrophy highlight the need for systemic therapies which restore SMN throughout the body.

Treatment

To date, the gold standard treatments for SMA has been to restore the levels of SMN protein throughout the body. To achieve this, current treatment options work to modify splicing of *SMN2* pre-mRNA or SMN gene replacement therapy ultimately resulting in increased expression of SMN. To date, there are three FDA approved medications for the treatment of SMA; nusinersen (Spinraza),[28] onasemnogene abeparvovec-xioi (Zolgensma) and risdiplam (Evrysdi). Each possess a unique method to improve symptom management and disease progression.

One of the first FDA approved drugs available to SMA patients was nusinersen (Spinraza) approved in 2016.[28] This anti-sense oligonucleotide works to increase the levels of functional SMN protein produced by the less efficient *SMN2* gene. Nusinersen acts through hybridizing to the intronic splicing silencer N1 region in intron 7 (ISS-N1) of *SMN2*. It blocks splicing, which promotes the inclusion of exon 7 and production of full length SMN.[28]

Another method utilized in increasing functional SMN protein in the body is the administration of onasemnogene abeparvovec-xioi (Zolgensma). This is a gene therapy that introduces the nonreplicating adeno-associated virus 9 (AAV9) carrying a functional *SMN1* cDNA throughout the CNS and periphery.[29] Administration of this gene therapy subsequently increases levels of functional SMN protein. Fortunately, onasemnogene is able to achieve these therapeutic benefits after only one intravenous dose.[29]

Finally, the most recent advancement of treating SMA was the development of risdiplam (Evrysdi). Like nusinersen, risdiplam acts as a *SMN2* pre-mRNA splicing modifier. Unlike nusinersen however risdiplam is a small molecule drug which attaches to the 5’ splice site

of intron 7 and to exonic splicing enhancer 2 in exon 7.[30] This then allows the production of more functional SMN from the *SMN2* gene. Risdiplam is currently the only SMA therapeutic available which uses the convenient oral administration method.[30]

In general, the primary goals of current SMA therapeutics are to increase the levels of functional SMN protein biologically available.[31] They share commonalities in their time-dependant administration, meaning the earlier the treatments are administered the more optimal the prognosis. They do however differ in their methods of administration (i.e., intrathecal injection, intravenous injection, and oral administration respectively) as well as dosage requirements. Overall, widespread replenishing of SMN protein is necessary for treatment given the protein's diverse functions in both the central nervous system and peripheral organs.

In addition to SMN restorative therapies, it is important to develop and explore novel non-SMN mediated therapies for the treatment of SMA. While SMN restoring treatments are essential in the treatment of CNS tissues in SMA, we have now well established that SMN depletion effects wide ranges of peripheral tissues as well. SMN depletion throughout the embryonic and infancy periods of life produce under characterized damage lasting throughout life. Given this, long term treatment of SMA patients require supportive therapies not limited to the restoration of SMN. For example, several SMN-independent therapies are in pre-clinical and clinical phases of research to improve muscle growth, differentiation, strength, and overall motor function.[32] Drugs in clinical trials include Reldesemtiv and SRK-015, and both have shown some success.[32] Overall, the development of SMN-independent therapies are essential in the long term support of SMA patients.

1.4 The Role of IGF-1 in SMA Pathology

Insulin-like growth factor I (IGF-1) is a pleotropic hormone involved in muscle growth, protein synthesis and homeostasis, as well as cell proliferation.[33] In addition to these functions, IGF-1 has also been shown to promote axonal outgrowth and elongation within corticospinal motor neurons, suggesting a novel therapeutic target in the treatment of multiple neurodegenerative conditions.[34] In this section, IGF-1 synthesis, mechanisms of action, and roles as a supporting therapy in SMA will be discussed.

Insulin-like Growth Factor 1 Biogenesis

IGF-1 synthesis begins primarily in the liver, where the stimulation by growth hormone (GH) from the anterior pituitary results in the secretion of mature IGF-1 into the blood stream. Beforehand, the pre-pro forms of IGF-1 produced by the *Igf-1* gene undergo several post-translational modifications prior to maturation and secretion. Beginning as an immature precursor protein, the protein generated from *Igf-1* mRNA consists of a signal peptide, mature IGF-1, and C terminus E peptide.[35] The signal peptide is initially cleaved in the endoplasmic reticulum (ER) after translation, and the E peptide may later be cleaved. Interestingly, little is known about these E peptides and immature pro-IGF-1 has been detected in the serum. It is hypothesized that pro-IGF-1 in the serum may be a biologically inactive form of these two peptides and a source of storage.[35] Once released into the serum, mature IGF-1 exerts various effects on nearly every tissue in the body. From cell proliferation and growth promotion to protein synthesis, a more in depth understanding of its mechanism of action better highlights its critical role.

Mechanism of Action of IGF-1

To achieve these functions, IGF-1 acts on a cell surface tyrosine kinase receptor to elicit a downstream cascade. This receptor, labeled the Insulin-like Growth Factor Receptor (IGF-1R) is widely expressed throughout the body, including in the muscle and CNS.[36] While IGF-1 can also interact with the Insulin Receptor (IR), this is done at a much lower affinity.[37] Nonetheless after the activation of IGF-1R, an IGF-1/Akt/mTOR pathway ensues to promote muscle growth and protein synthesis. This pathway is heavily regulated by various factors such as oxidative stress, amino acid availability, and inflammatory cytokines which all may halt this process. Given these roles in muscle growth, IGF-1 is an appealing therapeutic in the field of muscle wasting conditions such as SMA.

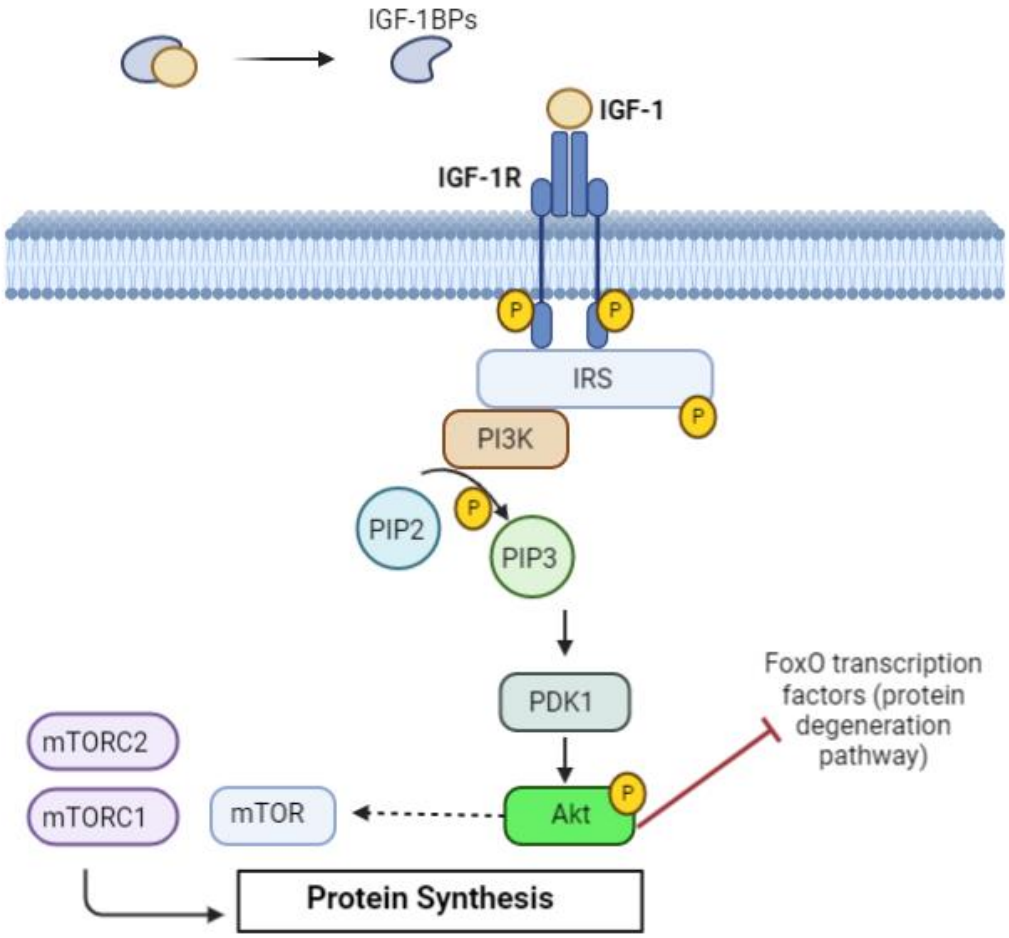

Figure 3. IGF-1 Mechanism of action in the stimulation of protein synthesis. IGF-1 activates its IGF-1R releasing a cascade of kinases, ultimately resulting in the phosphorylation of Protein Kinase B (Akt). This kinase indirectly interacts with mTOR, a mediator of growth, to promote protein synthesis and growth. Created with BioRender.

IGF-1 in Disease Modifying Therapies

Within SMA, several pathologies related to the absence or misfunction of IGF-1 have been identified within both patient and mouse models of the disease. To fully understand IGF-1 as a novel therapeutic target, we will first discuss these defects in more detail and how SMN and IGF-1 therapies work to correct these damages.

IGF-1 Defects in SMA Mouse and Patient Models

Throughout the literature, multiple studies have highlighted the IGF-1 defects observed as a downstream effect of SMN depletion. For example, mouse models of severe SMA have noted a generalized reduction of IGF-1 in blood plasma and liver.[24,38] In addition, there are also reported downregulation of Insulin-like growth factor binding protein acid labile subunits (Igfals), a protein involved in binding IGF-1 in the serum.[39] Interestingly, the binding protein responsible for carrying and regulating IGF-1, Insulin-like Growth Factor Binding Protein 3 (IGFBP3), remained unchanged throughout.[39] When a clinical study analyzed serum contents from 15 SMA patients, they reported that IGF-1 was decreased in patient serum while IGFBP3 was unchanged.[40] Further research on the patient population revealed that insulin resistance may actually be more associated with IGF-1 status than thought, with more insulin resistant patients possessing increased IGF-1 levels than insulin sensitive.[41] Contradicting previous research, this study found normal IGF-1 levels in patient serum when compared to health age, sex, and

pubertal stage controls. Finally, results from patient skeletal muscle biopsy demonstrate an overexpression of IGF-1R only in SMA Type I patients as compared to Type III.[42] Overall, many changes to the IGF-1 signaling cascade have been documented in various models of SMA. Each of these findings suggest impairment of IGF-1 bioavailability and downstream effects are present, particularly in the most severe form of the disease. To combat this, several investigations have tested IGF-1in a therapeutic context.

IGF-1 as a Therapy for SMA

Many studies have commonly investigated IGF-1in mice by two methods: IGF-1 protein administered as a treatment or effect on IGF-1 levels when given a gold standard SMN enhancing treatment. The first genre of study works to directly increase the levels of IGF-1 protein in the body or in specific tissue types by methods such as via recombinant vectors or localized administration of IGF-1 transgenes. For instance, an investigation which used AAV1 mediated introduction of the human IGF-1 gene systemically at P1 recorded increased motor function, body weight, innervation, decreased MN death, degree of muscle atrophy, and prolonged survival in the Taiwanese model's SMA effected mice.[43] Interestingly, when AAV2 mediated expression of hIGF-1 was restricted to the CNS in mild mouse models, they observed a rescue of MNs which failed to create axons capable of innervating muscle.[44] NMJs presented abnormally, and motor function in general was not rescued.[44] In a similar manner, when IGF-1 was restricted to the skeletal muscle of severe SMNΔ7 mice, overall survival improved and muscle fibre size increased however motor function was still impaired.[45] In general, IGF-1 therapy studies suggested that a systemic route of administration would demonstrate the most optimal outcomes.[43,44,46] The second area of study uses treatments commonly found in the treatment of SMA patients to increase levels of SMN protein. Subsequently, IGF-1 protein is

measured as a secondary effect of this. For example, it was observed in the Taiwanese model that when *SMN2* mis-splicing was corrected through the use of ASOs, both SMN, IGF-1 and Igfals levels increased in the serum to functional levels.[39]

In conclusion, IGF-1 related defects are reported in both animal and patient models of SMA as a downstream effect of SMN depletion. A variety of IGF-1 enhancing therapies have been developed and have demonstrated some therapeutic benefit by improving prognosis, restoring some motor function, and improving degree of muscle atrophy. This supplemental therapy for SMA could be beneficial when administered systemically and deserves further investigation for future patients.

1.5 Pathways of Tissue degeneration in SMA

As a result of denervation, intrinsic muscle defects, and SMN depletion, tissue degeneration is a common feature of SMA. Unfortunately, pathways in which specific tissues undergo degeneration remain elusive. For instance, pathways in which motor neurons perish and skeletal muscle atrophies remain under characterized in the current field of SMA. To better comprehend the molecular landscape of the disease, and subsequently develop more targeted therapies, one must review the current literature of tissue degeneration pathways and how these may be involved in SMA.

p53 Repair and Apoptosis Pathways

p53 is a well understood tumor suppressor protein which carries vital roles in determining cell fate. Via autophagy, apoptosis, and DNA repair pathways among others, p53 possess the ultimate task of preventing aberrant cell growth.[47] Thus, this ‘Guardian of the Genome’ acts

upon nearly every tissue in the body to arrest the cell cycle when damage occurs and allows pathways of repair or cell death to occur.

The first pathway refers to the repair of a damaged cell injured by stressors such as oxidative stress, mitotic stress, DNA strand breaks, and UV radiation damage. Dependant on the type of damage experienced, varying cascades may be activated to elicit cell repair. For instance, in the case of DNA damage, p53, which typically remains at a low-level baseline in the cell, becomes phosphorylated to increase stability.[48] Once phosphorylated, Mdm2, its negative regulator, is displaced and allows an accumulation of p53 to promote cell cycle arrest via p21.[48] Here, DNA damage may be mediated through nucleotide excision repair, base excision repair, or mismatch repair.[49] In a similar manner, p53 may also contribute to the repair of cells due to mitochondrial stress. For example, one study has shown that in response to muscle denervation, decreased mitochondria are observed in muscle fibres. They demonstrated via a muscle specific p53 KO mouse model that p53 facilitated the response to denervation damage and subsequent mitochondrial decline through regulating mitochondrial quality control pathways.[50] Overall, p53 is capable of arresting the cell cycle to mediate genotoxic or generalized cell stress to elicit repairs. However, should the damage be too extensive, p53 expands its role to incorporate autophagy and apoptosis.

The intrinsic apoptosis pathway mediated by p53 is vital in the removal of critically injured cells. To achieve this, upregulated phosphorylated p53 directly binds to DNA and acts as a transcription factor to induce the expression of BH3-only proteins (NOXA, PUMA).[51] In response, these proteins then inhibit pro-survival proteins (BCL-2 family) which allows a derepressing of apoptosis effectors (BAX, BAK).[51] Ultimately, this results in an increased

mitochondrial outer membrane permeability and cytochrome C release. The apoptosome is formed and a cascade of caspases complete the task of cell demolition.[51]

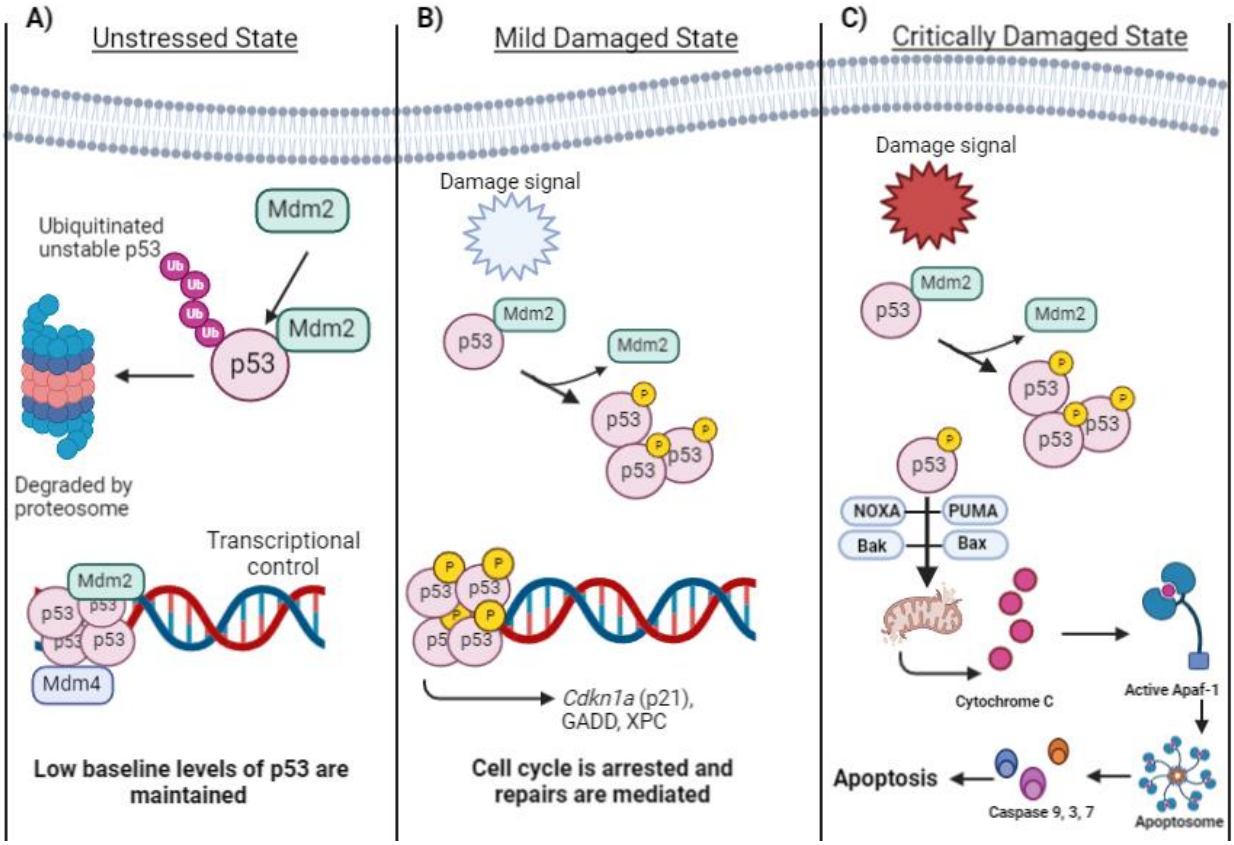

Figure 4. p53 mediates differential responses in the event of cellular damage. A) In unstressed states, p53 is non-phosphorylated and regulated by Mdm2. Mdm2 tags circulating p53 for destruction by the proteosome via ubiquitination and transcription is controlled. B) With mild damage, p53 becomes phosphorylated and stabilized by protein kinases, and encourages transcription of several downstream factors such as *Cdkn1a*, *GADD*, and *XPC* whose products are involved in cell cycle arrest (p21) and DNA repair. C) Critical damage to the cell results in p53's transcription of cell cycle arrest factors (*Cdkn1a*) as well as pro-apoptotic factors which create NOXA, PUMA, Bax and Bak (BH3-Only proteins). The outer mitochondrial cell

membrane ruptures releasing cytochrome c, which in turn promotes the formation of the apoptosome and subsequent caspase cascade leading to apoptosis. Created by BioRender.

In conclusion, p53 plays an important function in the repair or removal of cell types throughout the body. Utilizing their respective pathways, p53 can dictate cell fate in response to damage, as well as acting in response to denervation specifically. Given this recent evidence, p53 has been investigated within the context of SMA as a pathway of tissue degeneration.

p53 Mediated Apoptosis in SMA

Recent advance in the ongoing search for cell death and atrophy pathways in SMA has led researchers to study the association between SMN depletion and the presence of p53 mediated effects. In the end, it was uncovered that p53 and SMN directly interact, and select tissue types showed specific vulnerability to p53 mediated apoptosis. While the literature remains incomplete in this area, one can begin to understand the role of p53 in the most severe models of SMA disease.

To establish the relationship between SMN and p53 in the literature, a variety of immunoprecipitation, immunohistochemistry, and biomolecular interaction analysis were completed. These results indicated that FL-SMN binds directly to p53 within its Lysine rich domain, in both *in vivo* and *in vitro* models.[52] Curiously, SMA patient-derived mutations of SMN resulted in a decreased interaction between SMN/p53 and a failure to co-localize together within the CBs of the cell.[52] The study concluded that perhaps a failure in SMN/p53 interaction in SMA models could promote p53 mediated apoptosis in MN specifically. Therefore, the genomic profiles were compared between vulnerable versus more resistant MNs in a severe SMA mouse model. Strikingly, it was observed that phosphorylated p53 accumulated in

vulnerable MN more rapidly than resistant, however both groups demonstrated this accumulation.[53] When treatments blocking the transcription of p53 were administered, vulnerable MN loss was prevented.[53] Similarly, NMJ pathology onset occurred in conjunction with an increase in p53 related transcripts in the cell body.[54] In general, this implied that NMJ loss may be a p53 dependant process. When p53 was reduced in the model, NMJ loss was attenuated, however NMJ pathology, MN loss, and motor impairment were still observed.[54]

Contradictory evidence involving p53's role in MN and tissue degeneration has also been highlighted in severe SMA mouse models. For example, there was an observed upregulation of p53 in MNs, however not in whole spinal cord lysate of *Smn*$^{2B/-}$ mice.[55] When *Trp53* and *Cdkn1a* were systemically knocked out, survival was impaired, motor unit loss continued, and motor deficits were sustained. In general, it was proposed that neuronal death in the spinal cords of *Smn*$^{2B/-}$ mice occurred through a p53-independent mechanism.[55]

Overall, a range of evidence has provided insight to a possible role of p53 involvement in MN loss within SMA effected mouse models. Contradicting findings in the field are thus indicative of a need for further investigation to truly understand neuronal and tissue degeneration in SMA. More research in models of mild SMA and in various extra-neuronal tissues are required to understand the impacts of SMN truncation and depletion on p53 levels and subsequent pathways.

1.6 Research Methods and Aims

The Kothary laboratory has highlighted that CNS and extra-neuronal effects of SMN depletion occur throughout a severe model of SMA (*Smn*$^{2B/-}$). Due to the critical splicing functions attributed to SMN, multiple tissue types have previously been demonstrated to show impairments downstream of SMN. Given the importance of early therapeutic interventions in SMA, there remains a persistent need for the development of interventions which act independently of SMN. Investigation of *Igf-1* and p53 in various tissue types throughout disease progression will provide insights to novel therapeutic targets.

Aims:

1 Characterize mRNA transcript and protein levels of *Trp53* and *Igf-1* in the *Smn*$^{2B/-}$ model of severe SMA systemically and throughout disease progression.

2 Investigate and compare mRNA transcript and protein levels of *Trp53* and *Igf-1* in the *Smn*$^{2B/-}$*; SMN2*$^{+/-}$ model of mild SMA systemically and throughout disease progression.

2. Methods

2.1 Animal Models and Care

The *Smn*$^{2B/-}$ mice were generated in our laboratory on a C57BL/6 background.[56] Overall survival of these mice ranges from 21-28 days. Additionally, a *Smn*$^{2B/-}$*;SMN2*$^{+/-}$ model was generated on an FVB background by crossing *Smn*$^{-/-}$*;SMN2* and *Smn*$^{2B/2B}$ mice.[12] These mice will experience normal survival alongside neuromuscular junction pathology, denervation, muscle atrophy and weakness. In general, *Smn*$^{2B/-}$*; SMN2*$^{+/-}$ model represents mild SMA subtypes. Mice were then sacrificed at a pre-symptomatic or symptomatic time point respective to the SMA model. Central nervous system tissue, heart, liver, and tibialis anterior muscle were collected at each respective time point. All mice were subjected to a 12 h light-dark cycle and given *ad libitum* access to food and water. All animal experiments were approved by the University of Ottawa Animal Care Committee in accordance with guidelines of the Canadian Council of Animal Care.

2.2 RNA Isolation, cDNA synthesis, and RT-qPCR

RNA was extracted using the RNeasy Mini kit (Qiagen, 74106) as per the manufacturer's protocol. In brief, 20-25 ug of flash frozen tissue (brain, spinal cord, heart, liver) was homogenized in 350-600 µl of “RLT Lysis Buffer” and centrifuged for 3 min at >8000xg. Supernatant was collected and added to equal volumes of 70% ethanol, then filtered through the RNeasy spin column. Two consecutive 700 µl washes of “RW1 Buffer " was followed by three 500 µl washes of “RPE Buffer” to remove salt by-products. Each wash was filtered through columns by centrifuges >8000xg for 15 sec each. To ensure excess salts and buffers were removed, columns were dry spun for 2 min with a clean collection tube. Finally, RNA was eluted

from the column filter by directly adding 30 µl RNase-free water and centrifuging for 1 min at >8000xg. This 30 µl eluent was repassed through the column a second time for maximal RNA concentration. Sample concentration was measured using nanodrop, with 280:260 and 260:230 ratios remaining within 1.75-2.25 absorbance to ensure pure, stable RNA product. For the extraction of the particularly fibrous TA tissue, the RNeasy Fibrous Tissue Mini Kit (Qiagen, 74704) was used according to the manufacturer's protocol.

Following RNA isolation, cDNA was synthesized using RT^2 First Strand Kit (Qiagen, 330401) according to the manufacturer's protocol. In short, 200 ng sample RNA was added to 2 µl "GE Buffer" to remove genomic DNA. RNase-free water was then added to bring total volume to 10 µl. This mixture was then incubated for 5 min at 42 ºC in an Eppendorf MasterCycler. After cycling and 1 min cooling on ice, a 10 µl master mix was added, which included 1 µl "Control P2 Buffer", 2 µl "RE3 Reverse Transcriptase Mix", 3 µl RNase-free water, and 4 µl of 5x "BC3 Buffer". Samples were then subjected to a second incubation of 15 min at 42ºC and 5 min at 95ºC. Once complete, cDNA was left to cool on ice for 1 min and given 91 µl RNase-free water for a final diluted product. Samples were stored at -20ºC for short-term storage, or -80ºC for long term storage.

To determine expression of various genes of interest at the mRNA level, RT-qPCR was used. Using Bio-Rad CFX Connect qPCR machine, 4 µl of cDNA was added to 16 µl of master mix, which consisted of 1 µl pre-optimized reverse/forward primer (Bio-Rad), 5 µl RNase-free water, and 10 µl SsoAdvanced Universal SYBR Green Supermix (Bio-Rad, 1725275). Each assay was performed in technical triplicates with biological sample sizes ranging from n = 3-6. The RT-qPCR protocol was performed as followed: 95ºC for 2 min; 40 cycles of 95ºC for 5 sec and 60ºC for 30 sec; 65ºC to 95ºC in increments of 0.5ºC for 5 sec. Fold changes were then

calculated using the ΔΔCt method, being normalized to beta actin (ActB) as an internal control. Genes of interest included *Igf-1, Uba1, Trp53, Cdkn1a, Pmaip1, Mdm2, Bbc3, Bcl-211, Bad,* and *Bax*.

2.3 Antibody and Western Blotting Optimization

To optimize total protein transfer onto membranes, a series of different transfer methods and gel acrylamide percentages were tested. Between semi-wet and wet transfer methods it was determined by total protein stain that wet transfers produced more consistent and abundant protein transfer. Additionally, between 10%, 12.5% and 15% acrylamide gels, 12.5% gels produced the best results.

A series of primary antibodies were also tested for strength and specificity of signal of target protein. In total, four primary antibodies were tested in the detection of p53 protein, which included p53ser15 (Cell Signalling, 9286), p53ser15 (Cell Signalling, 9284), p53ser9 (Cell Signalling, 9288) and p53total (Cell Signalling, 2524).

Finally, signal detection methods were optimized between Enhanced Chemiluminescence (ECL) and Odyssey fluorescence methods. The ECL technique is a highly sensitive horse radish peroxidase detection method used to visualize specific proteins on an immunoblot. Similarly, the Odyssey method utilizes a fluorescent antibody which is detected digitally. Blots were incubated in either 5% milk or Blocking Buffer for 1 or 2 h to determine blocking and detection methods which resulted in the least amount of non-specific signal. In conclusion, blocking for 1 h in Blocking Buffer and using Odyssey detection methods proved most efficient.

2.4 Protein Isolation and Western Blotting

Protein extraction involved the homogenization of tissue samples in lysis buffer which consisted of RIPA buffer (20 mM Tris-HCl, 150 mM NaCl, 1 mM Na2EDTA, 1 mM EGTA, 1% NP-40, 1% sodium deoxycholate, 2.5 mM sodium pyrophosphate, 1 mM beta-glycerophosphate, 1 mM Na3VO4, 1 µg/ml leupeptin) (Cell Signalling, 9806), phosphatase inhibitor (Sigma, 4906837001), protease inhibitor (Sigma, 04693159001), PMSF, and ddH_2O. Samples were centrifuged at 4ºC for 30 min and supernatant was collected in a clean Eppendorf tube. Samples were kept at -20ºC for short term storage or -80ºC for long term storage.

Calculation of protein concentration in each sample was performed with the Peirce BCA Protein Assay Kit (ThermoFisher Scientific, 23225) according to the manufacturer's protocol. Briefly, albumin standards were generated in technical triplicates and each unknown sample given technical duplicates in a 96-well microplate. To begin, 25 µl of unknown sample (5x diluted) or standard was added to their respective wells followed by 200 µl of "Working Reagent" (a mixture of 50 parts "BCA Reagent A" to 1 part "BCA Reagent B"). The plate was then incubated at 37ºC for 30 min. Once complete, a microplate reader was utilized to record the absorbance values given when measured at a wavelength of 560 nm. A standard curve was generated using the albumin standard absorbance values and known concentrations, and unknown sample concentrations were extrapolated from the curve. These values were adjusted by the dilution factor to give the final sample concentration.

Finally, western blotting was completed utilizing 12.5% acrylamide gels and Odyssey visualization method as described above. To begin, 40 ug of protein sample was transferred to a sterile Eppendorf tube with 4x Laemmli buffer. Samples were denatured at 96ºC for 3 min in a hot water bath. Gel electrophoresis was performed until loading marker (protein ladder) reached

the end of the gel, often taking 2 h at 100 V. The gel was then placed between blotting paper and transfer membrane and submerged in wet transfer buffer. Wet transfer was for 1 h at 120 V. Membranes were then blocked with either milk (ECL visualization method) or Odyssey blocking buffer (Odyssey visualization method) for 2 h at room temperature on a shaker plate. Finally, primary antibody and left to incubate overnight at 4ºC.

Visualization of membranes began with 3 x 5-min washes of TBS-T followed by the addition of HRP-linked (ECL) secondaries or fluorophore secondary antibodies (Odyssey). Secondary antibodies were incubated at room temperature on membranes with agitation for 1 h. A second round of 3 x 5-min washes of TBS-T was performed. For ECL methods, membranes were incubated in super ECL substrate to enhance signals and read by photo sensitive film, while Odyssey membranes were immediately read by the Odyssey spectrometer. Images were analyzed using ImageJ and Excel software.

2.5 IGF-1 ELISA

For the quantification of mature IGF-1 protein in tissue homogenate samples, the Mouse/Rat IGF-I/IGF-1 Quantikine ELISA Kit (R&D Systems, MG100) was utilized following the manufacturer's protocol. To begin, a serial dilution of IGF-1 Standard and a dilution of samples in calibrator diluent (5-6-fold) were made. This was followed by the addition of 50 µl Calibrator diluent added to each well, and subsequent 50 µl of control, standard, or sample. All standards, controls and samples were added in duplicate. A plate sealer was added to the top of the microplate and left to incubate for 2 h at room temperature with slight agitation (microplate shaker). Each well was then aspirated and washed 4x with 400 µl of wash buffer. Following washes, 100 µl of Mouse/Rat IGF-1 Conjugate was added to each well before covering with a fresh plate sealer and incubating for 2 h at room temperature on the microplate shaker. The

washing procedure was then repeated a second time before the addition of 100 µl of Substrate Solution to each well. This was left to incubate for 30 min on a benchtop with protection from light. Following incubation, 100 µl of Stop Solution was added to each well and the microplate was read with a microplate reader at 450 nm with a correction at 540 nm. A standard curve was generated to calculate the relative concentrations of each unknown sample. All measurements were then standardized against total protein concentration added previously calculated by BCA Assay.

2.6 Statistical Analysis

To outline results numerically, Prism 6 GraphPad software was utilized in all data analyses. Independent two-tailed t tests were conducted between $Smn^{2B/-}$ tissues and $Smn^{2B/+}$ heterozygous littermate controls for each timepoint (pre-symptomatic and symptomatic). For all analyses, $p<0.05$ was designated as the threshold of statistical significance. Asterisks symbolize the degree of significance as follows: *=$p<0.05$, **=$p<0.01$, ***=$p<0.001$, ****=$p<0.0001$.

3. Results

3.1 SMN protein is decreased in both the CNS and peripheral tissues of the *Smn$^{2B/-}$* mouse model of severe SMA, and moderately decreased in the *Smn$^{2B/-}$; SMN2$^{+/-}$* model of mild SMA.

To begin the study, a simple validation experiment was conducted to determine the levels of SMN protein in each tissue at their respective pre-symptomatic and symptomatic timepoints. For the *Smn$^{2B/-}$* model of severe SMA, brain, spinal cord, liver, heart, and tibialis anterior muscle were collected at P9 (pre-symptomatic) and P19 (symptomatic) timepoints. For the *Smn$^{2B/-}$; SMN2$^{+/-}$* model of mild SMA, the same tissues were collected at age 5 months (pre-symptomatic) and 15 months (symptomatic). Western blots were then completed to quantify levels of SMN protein in each tissue compared to heterozygous littermate controls. For a means of standardization, an internal of alpha tubulin was used to compare levels of SMN protein present to total protein loaded.

The severe *Smn$^{2B/-}$* mice displayed substantial decrease in SMN within the CNS (Figure 4) and peripheral tissues (Figure 5) at both P9 and P19. Similarly, the *Smn$^{2B/-}$; SMN2$^{+/-}$* mice also showed moderate decreases in SMN in all tissues (Figures 6 and 7) at ages 5 and 15 months as compared to their heterozygous littermates.

A)

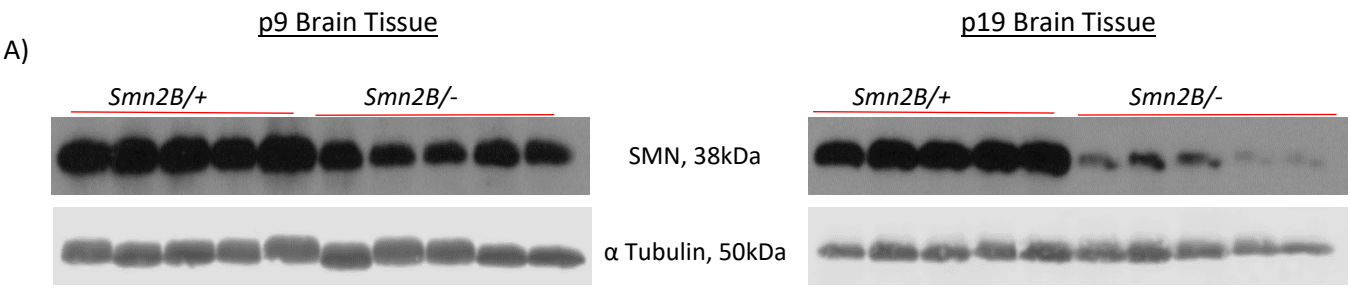
p9 Brain Tissue
p19 Brain Tissue
Smn2B/+
Smn2B/-
Smn2B/+
Smn2B/-
SMN, 38kDa
α Tubulin, 50kDa

B)

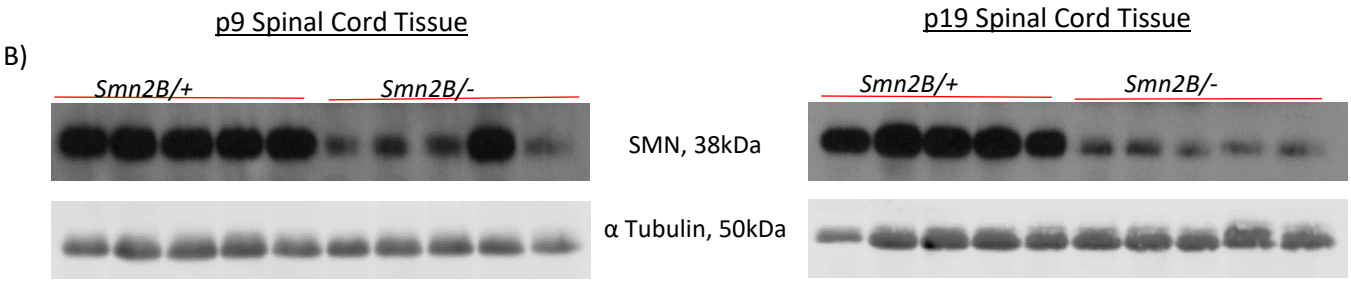
p9 Spinal Cord Tissue
p19 Spinal Cord Tissue
Smn2B/+
Smn2B/-
Smn2B/+
Smn2B/-
SMN, 38kDa
α Tubulin, 50kDa

C)

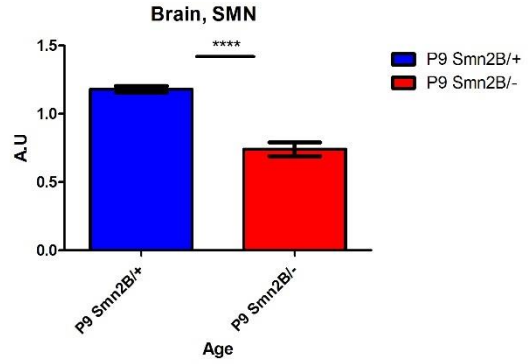
Brain, SMN
****
A.U
1.5
1.0
0.5
0.0
P9 Smn2B/+
P9 Smn2B/-
P9 Smn2B/+
P9 Smn2B/-
Age

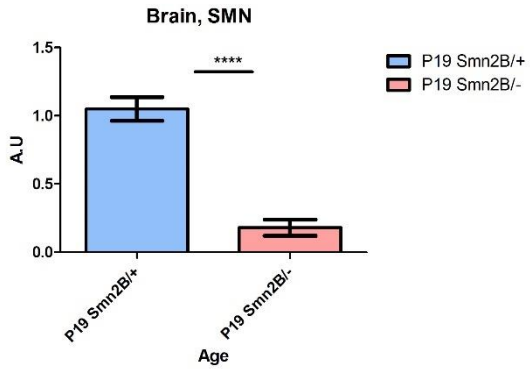
Brain, SMN
****
A.U
1.5
1.0
0.5
0.0
P19 Smn2B/+
P19 Smn2B/-
P19 Smn2B/+
P19 Smn2B/-
Age

D)

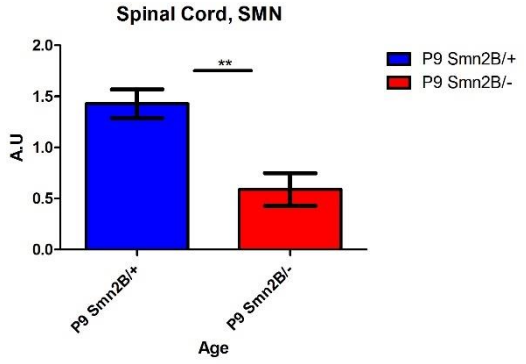
Spinal Cord, SMN
**
A.U
2.0
1.5
1.0
0.5
0.0
P9 Smn2B/+
P9 Smn2B/-
P9 Smn2B/+
P9 Smn2B/-
Age

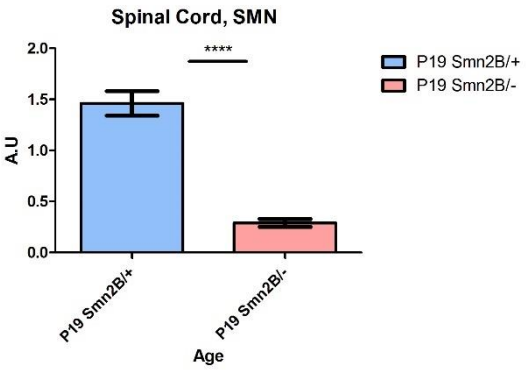
Spinal Cord, SMN
****
A.U
2.0
1.5
1.0
0.5
0.0
P19 Smn2B/+
P19 Smn2B/-
P19 Smn2B/+
P19 Smn2B/-
Age

Figure 5. SMN protein is significantly decreased in the CNS of *Smn*$^{2B/-}$ mice. Western blot analysis of anti-SMN signal detected by ECL visualization methods. Figure displays membrane images of brain (A) and SC (B) tissues throughout disease course. Signal intensity measured within p9 and p19 brain (C) and SC (D) compared to heterozygous controls. Values were standardized to alpha tubulin as internal control. Averages represent mean ± SEM, n=5, unpaired t test. *=$p<0.05$, **=$p<0.01$, ***=$p<0.001$, ****=$p<0.0001$.

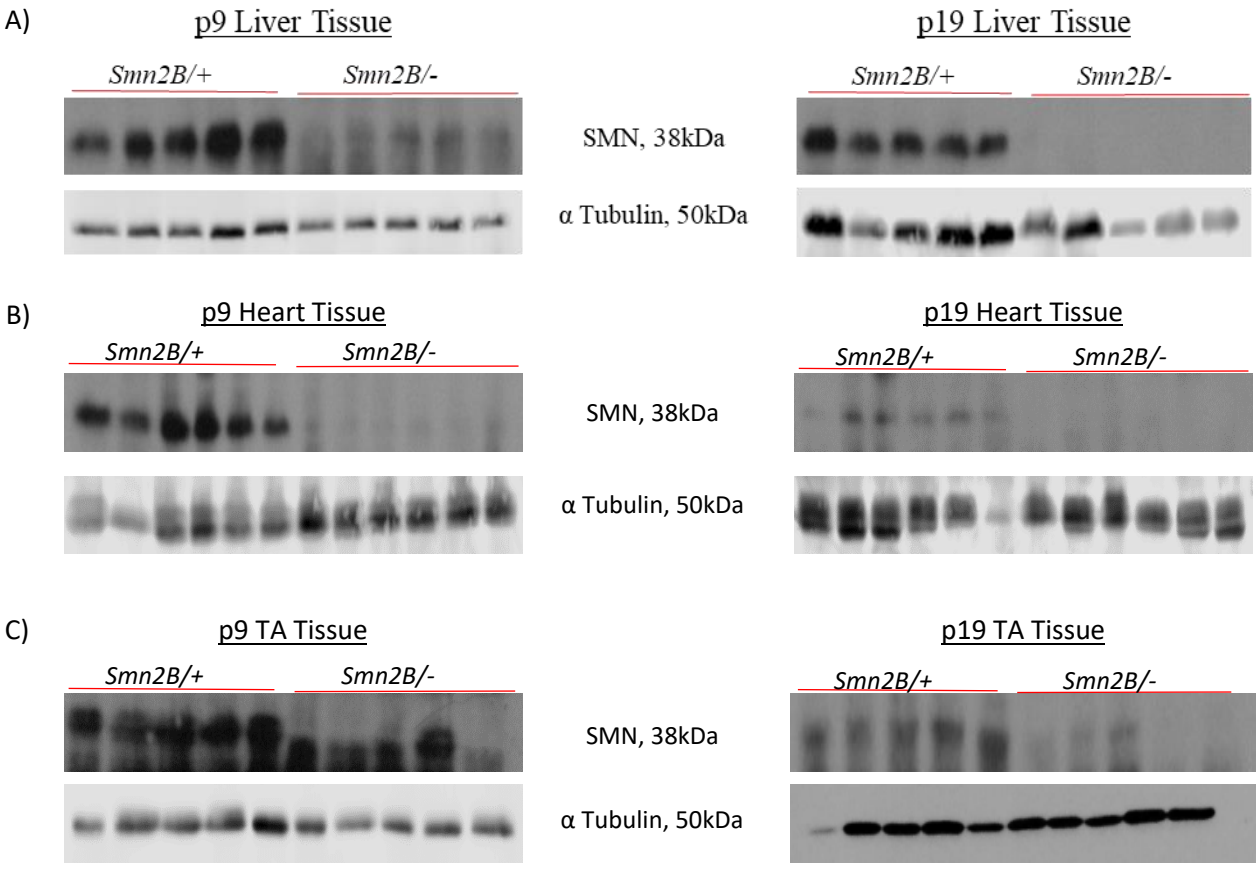
A)
p9 Liver Tissue
p19 Liver Tissue
Smn2B/+
Smn2B/-
SMN, 38kDa
α Tubulin, 50kDa
B)
p9 Heart Tissue
p19 Heart Tissue
C)
p9 TA Tissue
p19 TA Tissue

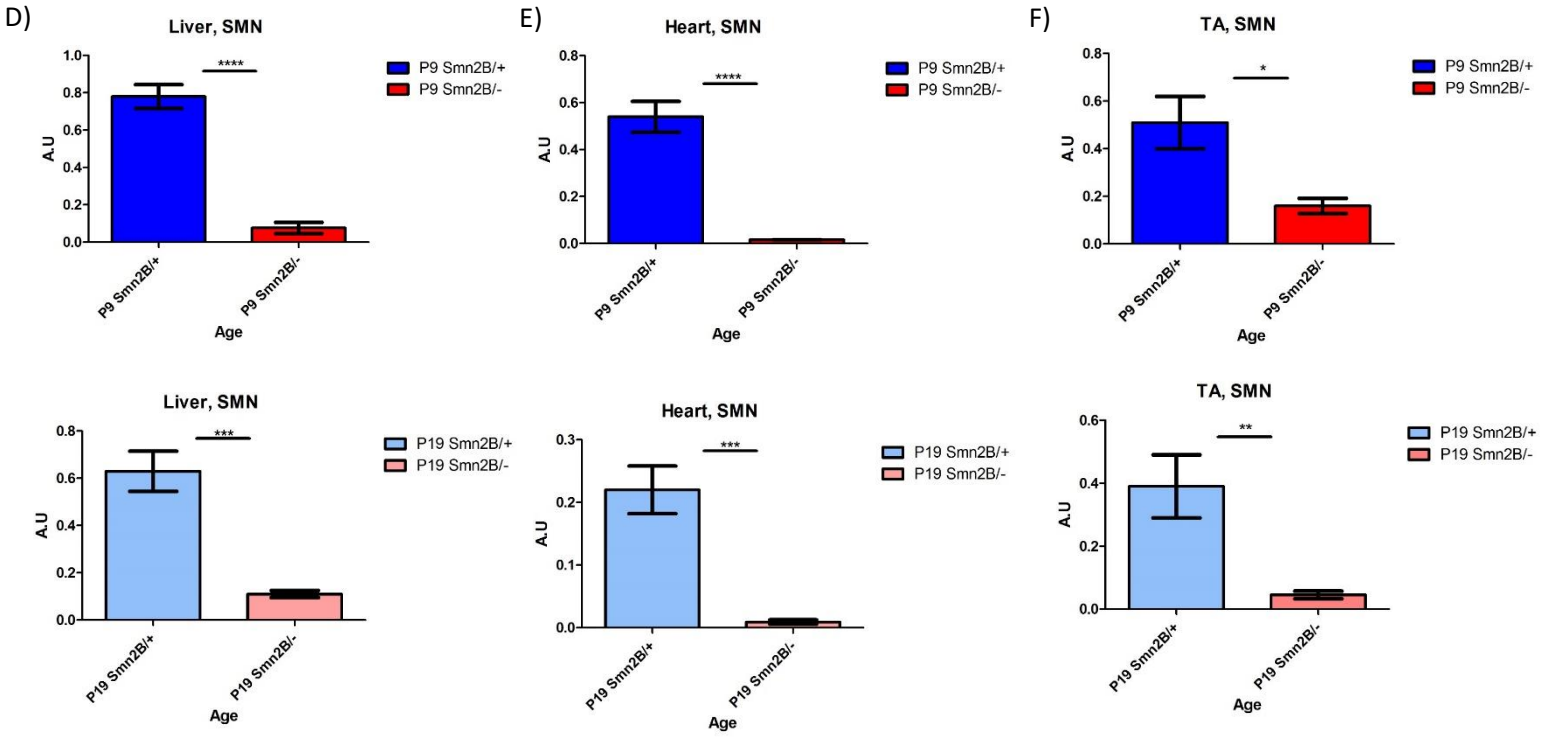
D)
Liver, SMN
E)
Heart, SMN
F)
TA, SMN
P9 Smn2B/+
P9 Smn2B/-
P19 Smn2B/+
P19 Smn2B/-
A.U
Age

Figure 6. SMN protein is decreased within peripheral organs of severe *Smn*$^{2B/-}$ mice. Western blot analysis of liver (A), heart (B), and TA muscle (C) at P9 and P19 compared to *Smn*$^{2B/+}$ littermate controls. Signal intensity values for liver (D), heart (E), and TA muscle (F) measured in arbitrary units and standardized to alpha tubulin internal control. Values represent mean ± SEM, n=5, unpaired t test. *=p<0.05, **=p<0.01, ***=p<0.001, ****=p<0.0001.

A)

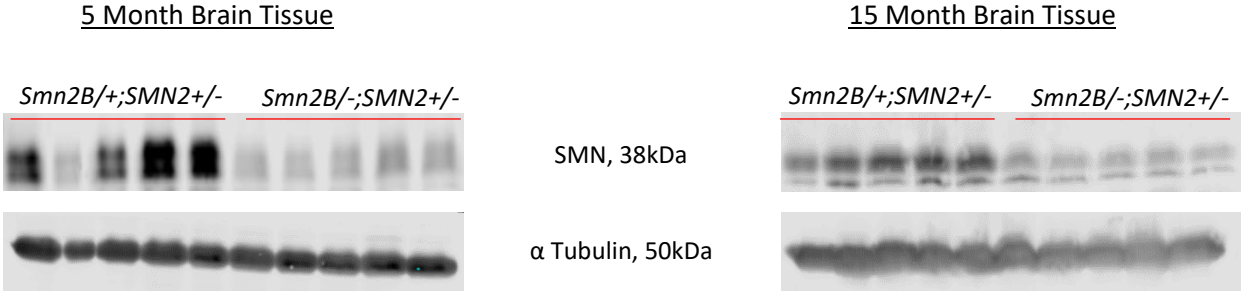
5 Month Brain Tissue
15 Month Brain Tissue
Smn2B/+;SMN2+/-
Smn2B/-;SMN2+/-
Smn2B/+;SMN2+/-
Smn2B/-;SMN2+/-
SMN, 38kDa
α Tubulin, 50kDa

B)

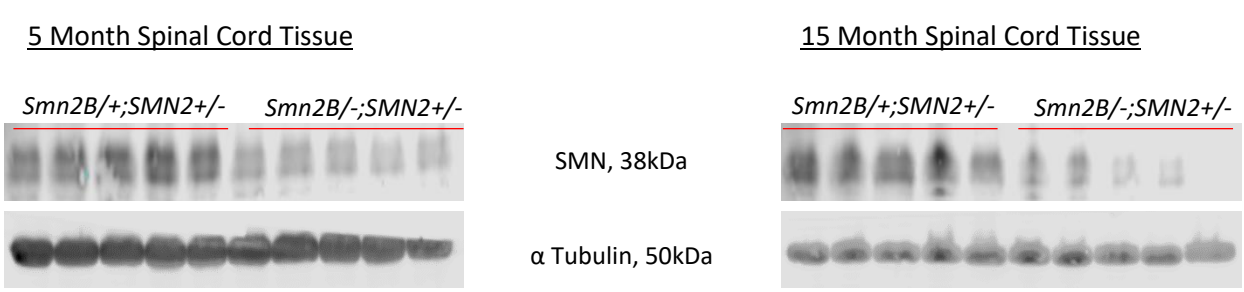
5 Month Spinal Cord Tissue
15 Month Spinal Cord Tissue
Smn2B/+;SMN2+/-
Smn2B/-;SMN2+/-
Smn2B/+;SMN2+/-
Smn2B/-;SMN2+/-
SMN, 38kDa
α Tubulin, 50kDa

C)

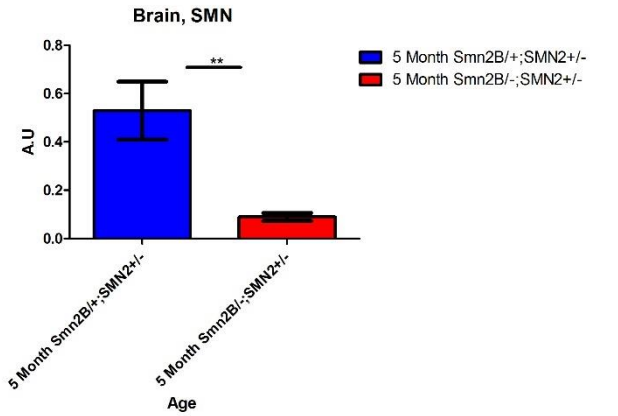
Brain, SMN
**
5 Month Smn2B/+;SMN2+/-
5 Month Smn2B/-;SMN2+/-
A.U
0.0
0.2
0.4
0.6
0.8
5 Month Smn2B/+;SMN2+/-
5 Month Smn2B/-;SMN2+/-
Age

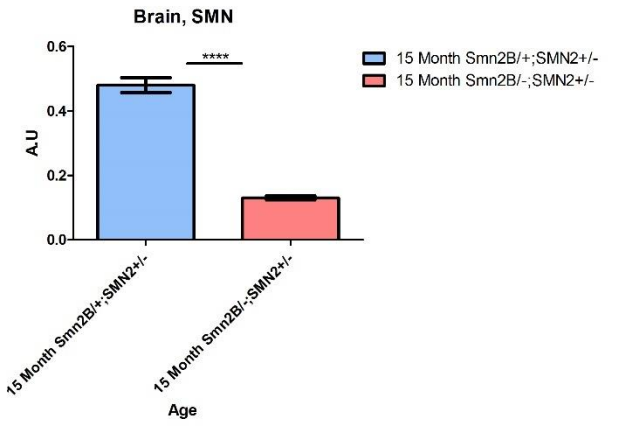
Brain, SMN
****
15 Month Smn2B/+;SMN2+/-
15 Month Smn2B/-;SMN2+/-
A.U
0.0
0.2
0.4
0.6
15 Month Smn2B/+;SMN2+/-
15 Month Smn2B/-;SMN2+/-
Age

D)

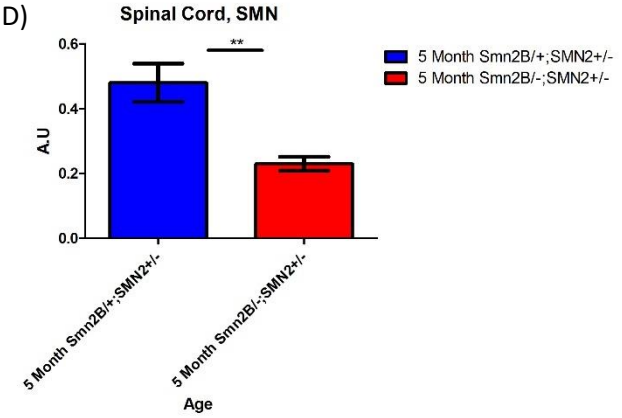
Spinal Cord, SMN
**
5 Month Smn2B/+;SMN2+/-
5 Month Smn2B/-;SMN2+/-
A.U
0.0
0.2
0.4
0.6
5 Month Smn2B/+;SMN2+/-
5 Month Smn2B/-;SMN2+/-
Age

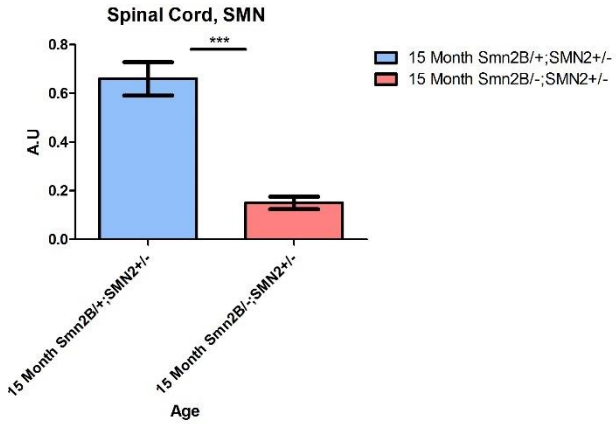
Spinal Cord, SMN
***
15 Month Smn2B/+;SMN2+/-
15 Month Smn2B/-;SMN2+/-
A.U
0.0
0.2
0.4
0.6
0.8
15 Month Smn2B/+;SMN2+/-
15 Month Smn2B/-;SMN2+/-
Age

Figure 7. SMN protein is decreased within CNS tissues of the *Smn$^{2B/-}$; SMN2$^{+/-}$* mouse model of mild SMA. Western blot analysis of anti-SMN signal detected by ECL visualization methods. Figure displays membrane images of brain (A) and SC (B) tissues at 5 months and 15 months. Signal intensity measured within 5-month and 15-month brain (C), and SC (D) tissues compared to *Smn^{2B+}; SMN2$^{+/-}$* heterozygous controls. Values were standardized to alpha tubulin as internal control. Averages represent mean ± SEM, n=5, unpaired t test. *=p<0.05, **=p<0.01, ***=p<0.001, ****=p<0.0001.

A)

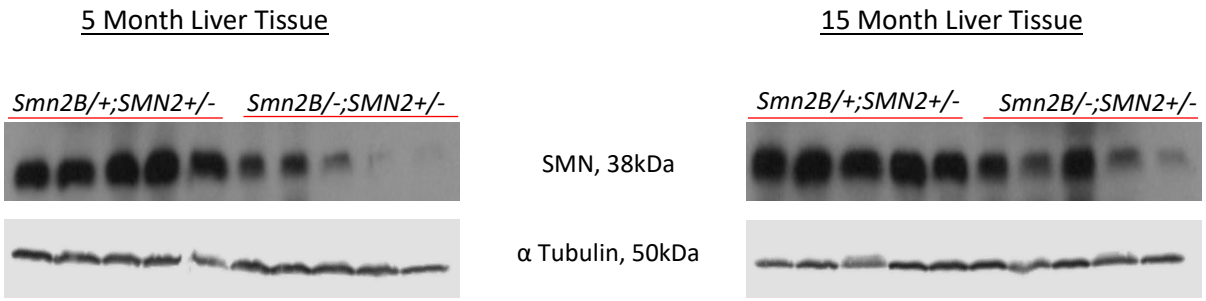
5 Month Liver Tissue
15 Month Liver Tissue
Smn2B/+;SMN2+/-
Smn2B/-;SMN2+/-
Smn2B/+;SMN2+/-
Smn2B/-;SMN2+/-
SMN, 38kDa
α Tubulin, 50kDa

B)

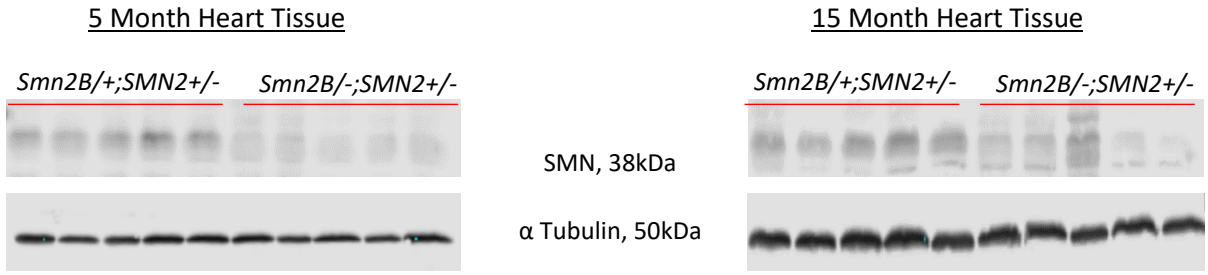
5 Month Heart Tissue
15 Month Heart Tissue
Smn2B/+;SMN2+/-
Smn2B/-;SMN2+/-
Smn2B/+;SMN2+/-
Smn2B/-;SMN2+/-
SMN, 38kDa
α Tubulin, 50kDa

C)

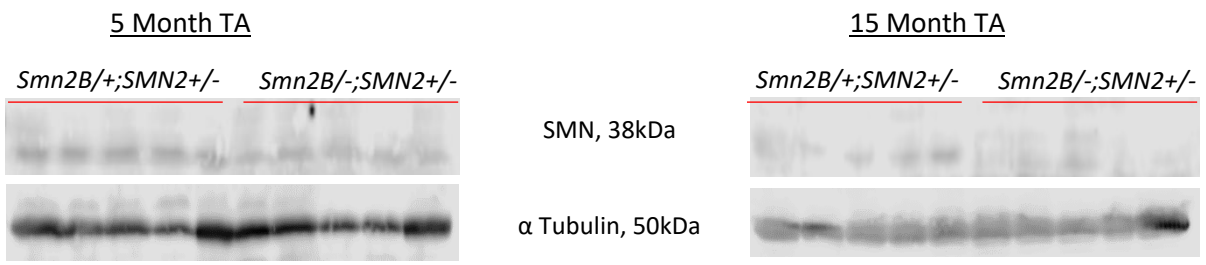
5 Month TA
15 Month TA
Smn2B/+;SMN2+/-
Smn2B/-;SMN2+/-
Smn2B/+;SMN2+/-
Smn2B/-;SMN2+/-
SMN, 38kDa
α Tubulin, 50kDa

D)

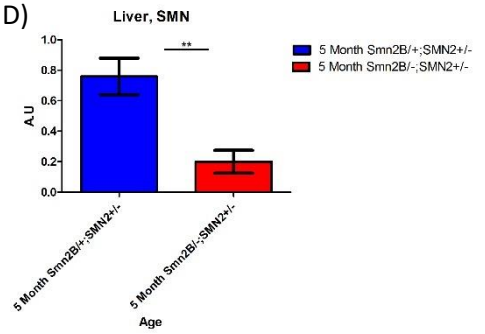
Liver, SMN
**
5 Month Smn2B/+;SMN2+/-
5 Month Smn2B/-;SMN2+/-
A.U
Age

E)

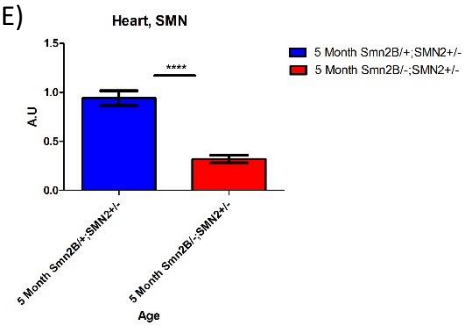
Heart, SMN
****
5 Month Smn2B/+;SMN2+/-
5 Month Smn2B/-;SMN2+/-
A.U
Age

F)

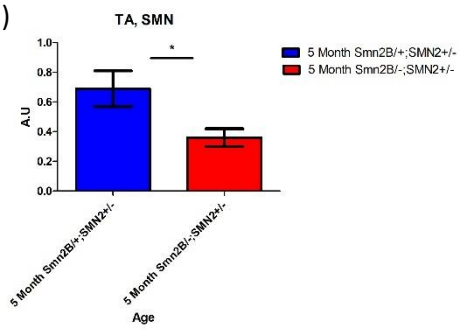
TA, SMN
*
5 Month Smn2B/+;SMN2+/-
5 Month Smn2B/-;SMN2+/-
A.U
Age

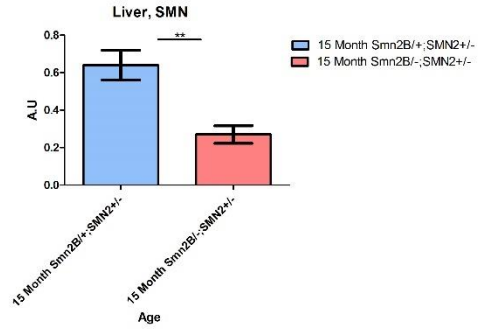
Liver, SMN
**
15 Month Smn2B/+;SMN2+/-
15 Month Smn2B/-;SMN2+/-
A.U
Age

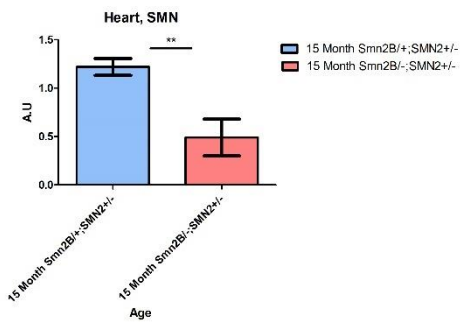
Heart, SMN
**
15 Month Smn2B/+;SMN2+/-
15 Month Smn2B/-;SMN2+/-
A.U
Age

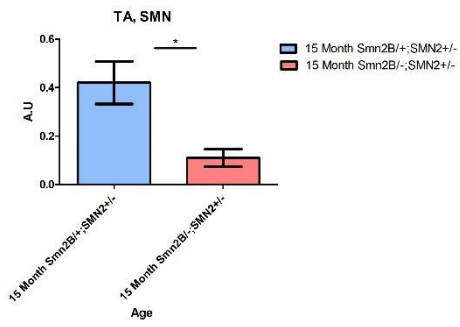
TA, SMN
*
15 Month Smn2B/+;SMN2+/-
15 Month Smn2B/-;SMN2+/-
A.U
Age

Figure 8. SMN is moderately decreased in the peripheral organs of the *Smn$^{2B/-}$; SMN2$^{+/-}$* mouse model of mild SMA. Western blot analysis of liver (A), heart (B), and TA muscle (C) throughout disease course compared to *Smn$^{2B/+}$; SMN2$^{+/-}$* littermate controls. Signal intensity values for liver (D), heart (E), and TA muscle (F) measured in arbitrary units and standardized to alpha tubulin internal control. Values represent mean ± SEM, n=5, unpaired t test. *=p<0.05, **=p<0.01, ***=p<0.001, ****=p<0.0001.

3.2 *Igf-1* mRNA levels are decreased in symptomatic livers of *Smn*$^{2B/-}$ mice, with a corresponding decrease in IGF-1 protein in peripheral organs.

To outline any possible changes in *Igf-1* mRNA expression or protein product generation, RT-qPCR and ELISA methods were utilized. *Smn*$^{2B/-}$ mice and heterozygous littermate controls were anesthetized at P9 and P19 postnatally and tissues flash frozen. Total RNA was extracted, and RT-qPCR was performed to determine the levels of *Igf-1* mRNA in each tissue normalized to beta actin transcripts as an internal control.

Within the *Smn*$^{2B/-}$ model, symptomatic mice experienced a stark downregulation of *Igf-1* mRNA within liver tissues (Figure 8C). Interestingly, *Igf-1* mRNA levels in other peripheral organs such as heart and TA muscle remained unchanged throughout the disease course (Figure 8E). Within the CNS, levels of *Igf-1* mRNA in brain tissue also remained unchanged at both the P9 and P19 timepoints (Figure 8A) while mild upregulation was observed in pre-symptomatic spinal cords compared to littermates (Figure 8B).

A)

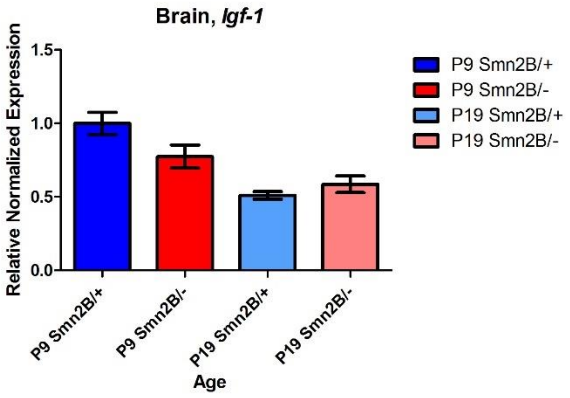
Brain, lgf-1
Relative Normalized Expression
1.5
1.0
0.5
0.0
P9 Smn2B/+
P9 Smn2B/-
P19 Smn2B/+
P19 Smn2B/-
Age
P9 Smn2B/+
P9 Smn2B/-
P19 Smn2B/+
P19 Smn2B/-

B)

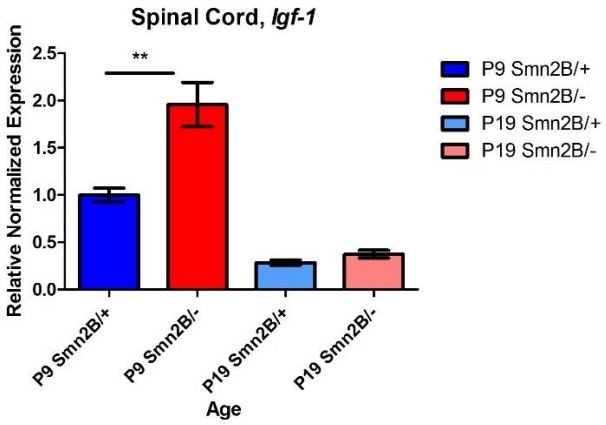
Spinal Cord, lgf-1
Relative Normalized Expression
2.5
2.0
1.5
1.0
0.5
0.0
**
P9 Smn2B/+
P9 Smn2B/-
P19 Smn2B/+
P19 Smn2B/-
Age
P9 Smn2B/+
P9 Smn2B/-
P19 Smn2B/+
P19 Smn2B/-

C)

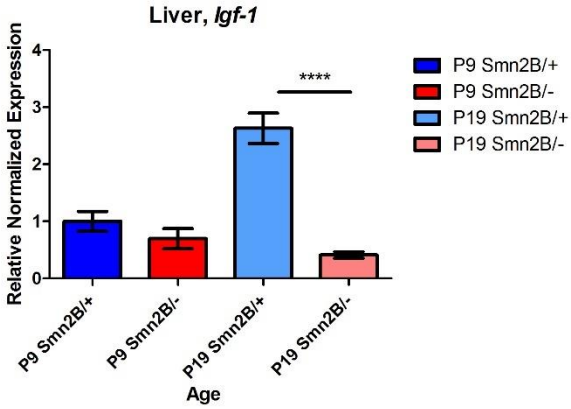
Liver, lgf-1
Relative Normalized Expression
4
3
2
1
0
****
P9 Smn2B/+
P9 Smn2B/-
P19 Smn2B/+
P19 Smn2B/-
Age
P9 Smn2B/+
P9 Smn2B/-
P19 Smn2B/+
P19 Smn2B/-

D)

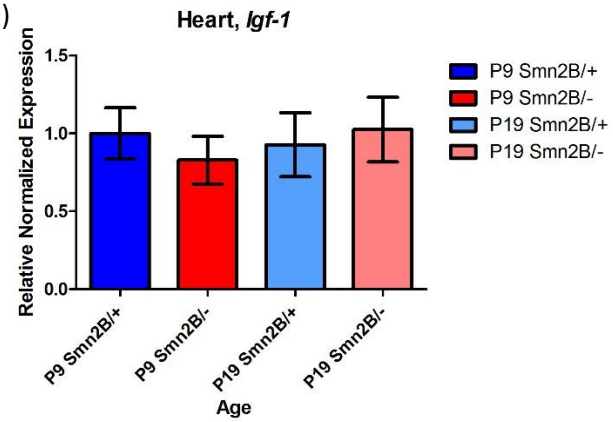
Heart, lgf-1
Relative Normalized Expression
1.5
1.0
0.5
0.0
P9 Smn2B/+
P9 Smn2B/-
P19 Smn2B/+
P19 Smn2B/-
Age
P9 Smn2B/+
P9 Smn2B/-
P19 Smn2B/+
P19 Smn2B/-

E)

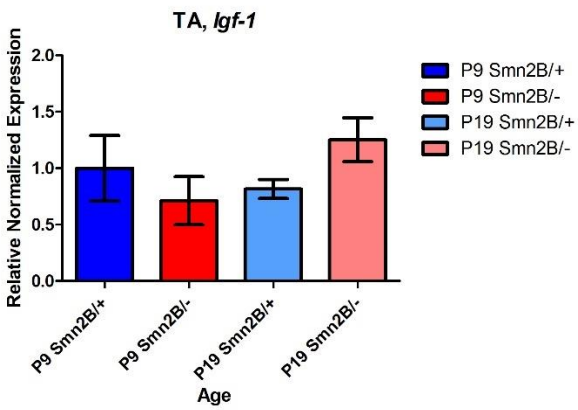
TA, lgf-1
Relative Normalized Expression
2.0
1.5
1.0
0.5
0.0
P9 Smn2B/+
P9 Smn2B/-
P19 Smn2B/+
P19 Smn2B/-
Age
P9 Smn2B/+
P9 Smn2B/-
P19 Smn2B/+
P19 Smn2B/-

Figure 9. *Igf-1* mRNA is substantially decreased within symptomatic liver tissues of the severe *Smn$^{2B/-}$* mouse model of SMA. RT-qPCR analysis compared relative *Igf-1* mRNA levels within brain (A), SC (B), liver (C), heart (D), and TA muscle (E) throughout disease course and compared to *Smn$^{2B/+}$* littermate controls. Values were normalized to *ActB* expression and represent mean ± SEM, n = 3-6, unpaired t test. *=p<0.05, **=p<0.01, ***=p<0.001, ****=p<0.0001.

We next wanted to determine the levels of IGF-1 protein product in each tissue. With the *Smn*$^{2B/-}$ mice, tissues were subjected to total protein extraction and IGF-1 levels determined by ELISA. The assay works as a solid phase sandwich assay, trapping and fluorescently labelling both free and IGF-1BP bound mature IGF-1 in each sample. These colorimetric results are then measured at a specific absorbance and compared to an IGF-1 standard curve. To normalize between wells, results were standardized to total protein concentration, previously determined by BCA assay.

It was determined that within the *Smn*$^{2B/-}$ mice, IGF-1 protein was significantly decreased in all peripheral tissues (heart, liver, and TA muscle) at the symptomatic timepoint compared to littermate controls (Figure 9C-E). Interestingly, the CNS did not show any change in IGF-1 protein levels at either time point (Figure 9A and B).

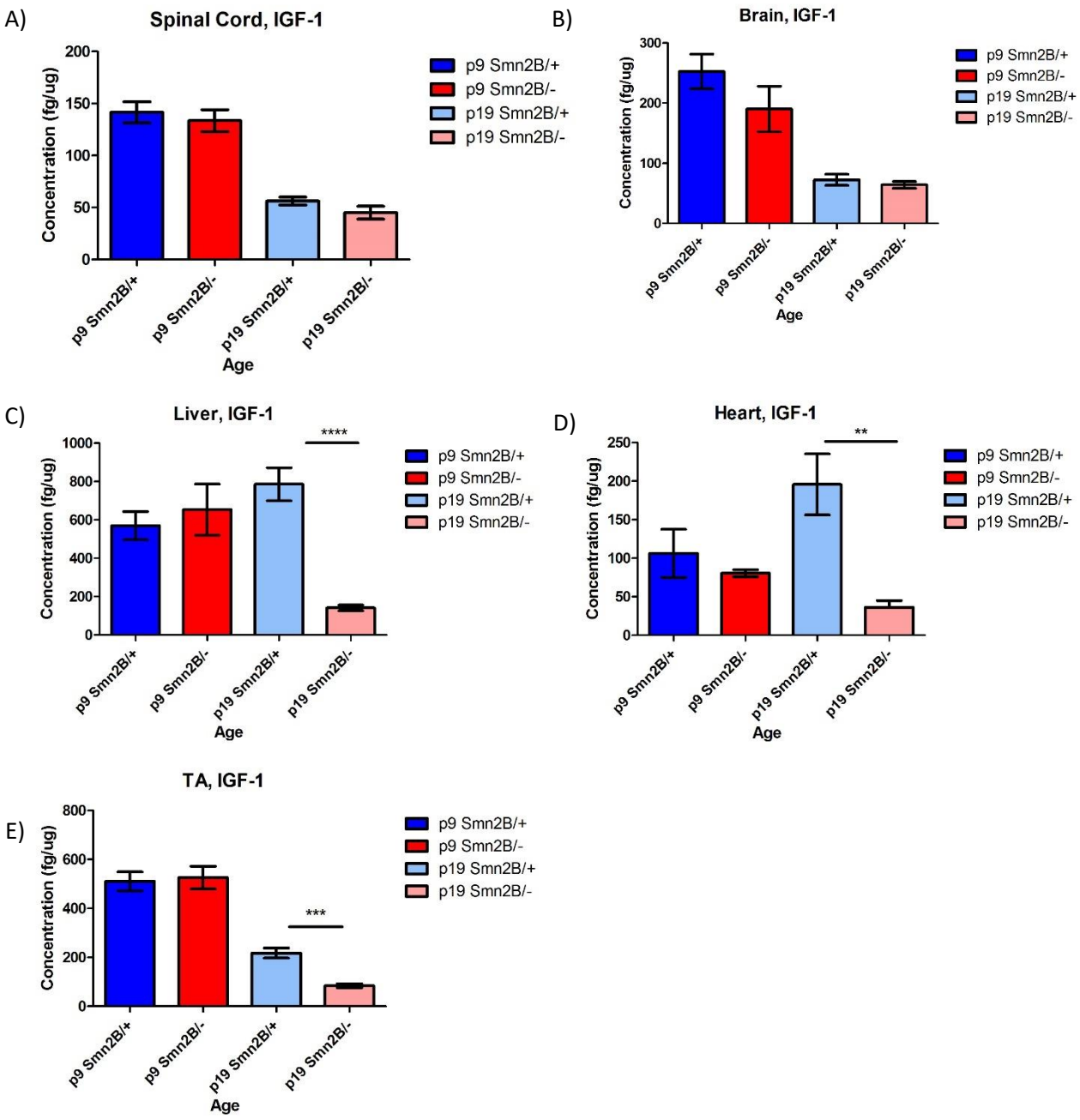

Figure 10. Mature IGF-1 protein product is significantly decreased in the peripheral organs of severe *Smn*$^{2B/-}$ mice. ELISA measurements displayed significant IGF-1 decrease in symptomatic peripheral tissues (C-E), but not in CNS tissue (A-B), as compared to *Smn*$^{2B/+}$ littermate controls. Values were normalized to total protein added per well and represent mean ± SEM, n= 5, unpaired t test. *=p<0.05, **=p<0.01, ***=p<0.001, ****=p<0.0001.

3.3 *Igf-1* mRNA and IGF-1 protein levels are minimally affected in the *Smn$^{2B/-}$; SMN2$^{+/-}$* model of mild SMA

The IGF-1 changes found in the severe *Smn$^{2B/-}$* mice raised the question if similar results would be detected in the mild *Smn$^{2B/-}$; SMN2$^{+/-}$* model of SMA. This model produces only moderate decreases of SMN protein throughout the body, and a mild phenotype overall. To begin, identical RT-qPCR methods were used to detect *Igf-1* mRNA expression at pre-symptomatic (5 months) and symptomatic (15 months) time points.

Within the mild model, there was a significant increase of *Igf-1* mRNA at the symptomatic timepoint within the liver (Figure 10C). However, no changes in *Igf-1* mRNA expression were observed at either timepoint in CNS tissues, heart, or pre-symptomatic TA muscle (Figure 10). Interestingly, *Igf-1* was decreased within symptomatic TA skeletal muscle (Figure 10E).

A)

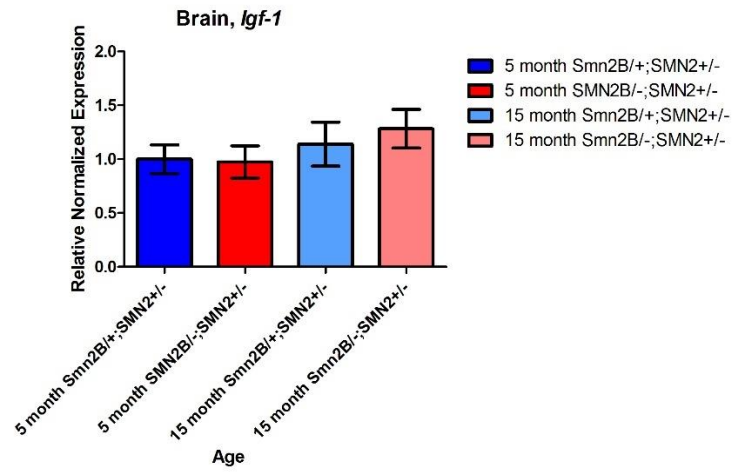
Brain, Igf-1
Relative Normalized Expression
2.0
1.5
1.0
0.5
0.0
5 month Smn2B/+;SMN2+/-
5 month SMN2B/-;SMN2+/-
15 month Smn2B/+;SMN2+/-
15 month Smn2B/-;SMN2+/-
Age

B)

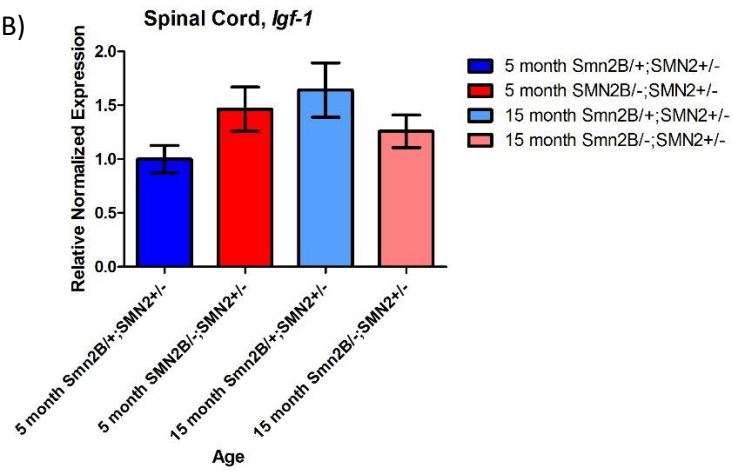
Spinal Cord, Igf-1
Relative Normalized Expression
2.0
1.5
1.0
0.5
0.0
5 month Smn2B/+;SMN2+/-
5 month SMN2B/-;SMN2+/-
15 month Smn2B/+;SMN2+/-
15 month Smn2B/-;SMN2+/-
Age

C)

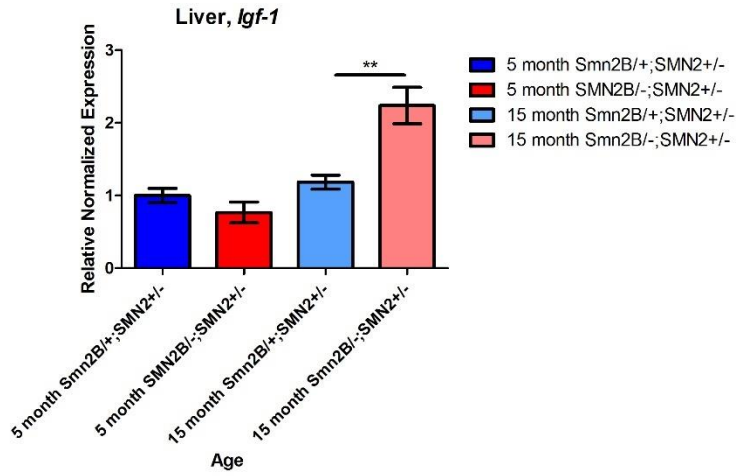
Liver, Igf-1
Relative Normalized Expression
3
2
1
0
**
5 month Smn2B/+;SMN2+/-
5 month SMN2B/-;SMN2+/-
15 month Smn2B/+;SMN2+/-
15 month Smn2B/-;SMN2+/-
Age

D)

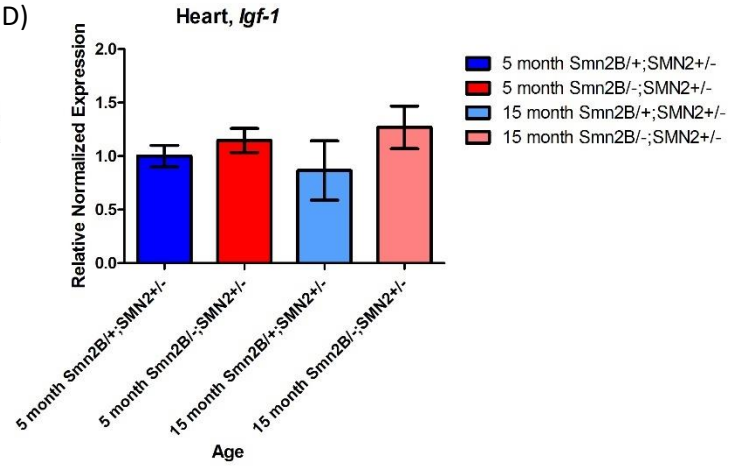
Heart, Igf-1
Relative Normalized Expression
2.0
1.5
1.0
0.5
0.0
5 month Smn2B/+;SMN2+/-
5 month Smn2B/-;SMN2+/-
15 month Smn2B/+;SMN2+/-
15 month Smn2B/-;SMN2+/-
Age

E)

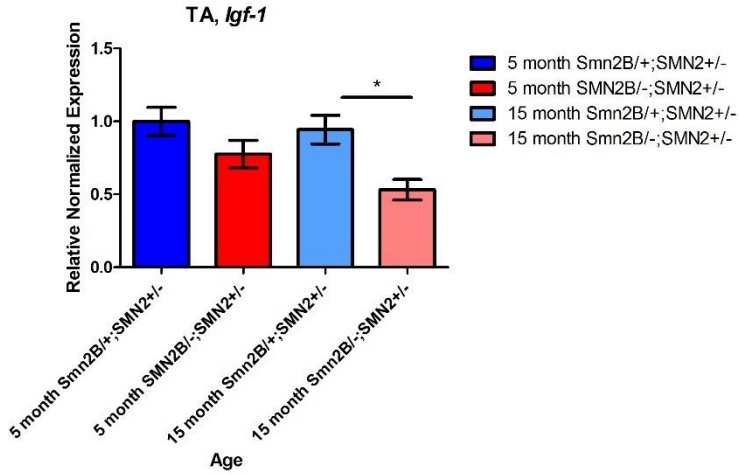
TA, Igf-1
Relative Normalized Expression
1.5
1.0
0.5
0.0
*
5 month Smn2B/+;SMN2+/-
5 month SMN2B/-;SMN2+/-
15 month Smn2B/+;SMN2+/-
15 month Smn2B/-;SMN2+/-
Age

Figure 11. *Igf-1* mRNA remains unchanged throughout disease course within the *Smn$^{2B/-}$; SMN2$^{+/-}$* mouse model of mild SMA. RT-qPCR analysis compared relative *Igf-1* expression levels within brain (A), SC (B), liver (C), heart (D), and TA muscle (E) throughout disease course as compared to heterozygous littermate controls. Values were normalized to *ActB* expression and represent mean ± SEM, n = 3-6, unpaired t test. *=p<0.05, **=p<0.01, ***=p<0.001, ****=p<0.0001.

Finally, we completed our IGF-1 study by quantifying levels of IGF-1 protein using the ELISA protocol. As discussed previously, brain, spinal cord, liver, heart, and TA muscle were collected at 5 and 15 months of age.

In heart and CNS tissues, no IGF-1 changes were observed throughout disease course (Figure 11A, B, D), while a slight decrease of protein was detected in pre-symptomatic liver (Figure 11C). Interestingly, there was an observed upregulation of IGF-1 protein in the symptomatic TA muscle (Figure 11E) despite the previously observed decrease of its mRNA.

A)

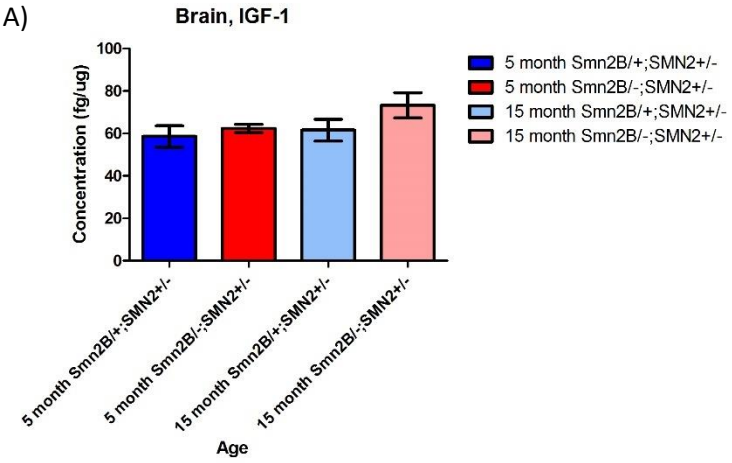
Brain, IGF-1
Concentration (fg/ug)
100
80
60
40
20
0
5 month Smn2B/+;SMN2+/-
5 month Smn2B/-;SMN2+/-
15 month Smn2B/+;SMN2+/-
15 month Smn2B/-;SMN2+/-
Age

B)

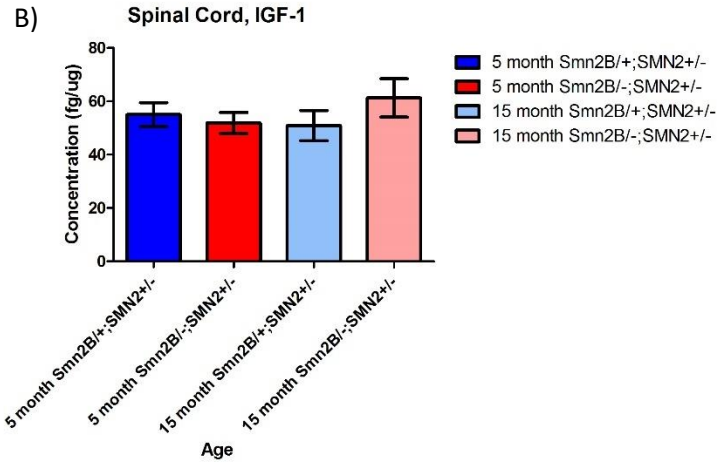
Spinal Cord, IGF-1
Concentration (fg/ug)
80
60
40
20
0
5 month Smn2B/+;SMN2+/-
5 month Smn2B/-;SMN2+/-
15 month Smn2B/+;SMN2+/-
15 month Smn2B/-;SMN2+/-
Age

C)

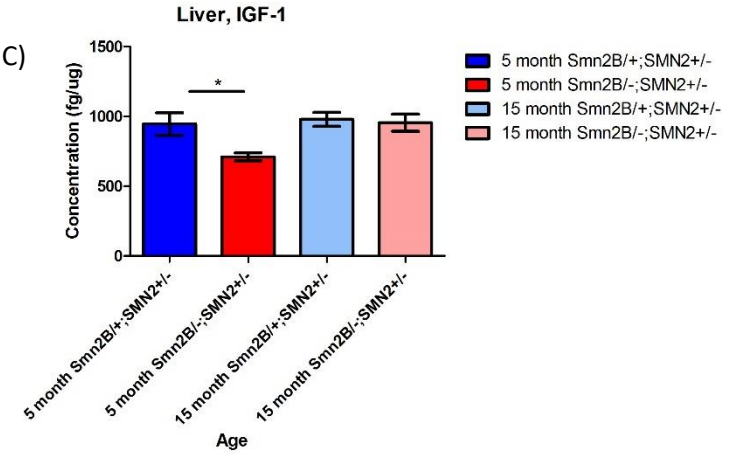
Liver, IGF-1
Concentration (fg/ug)
1500
1000
500
0
*
5 month Smn2B/+;SMN2+/-
5 month Smn2B/-;SMN2+/-
15 month Smn2B/+;SMN2+/-
15 month Smn2B/-;SMN2+/-
Age

D)

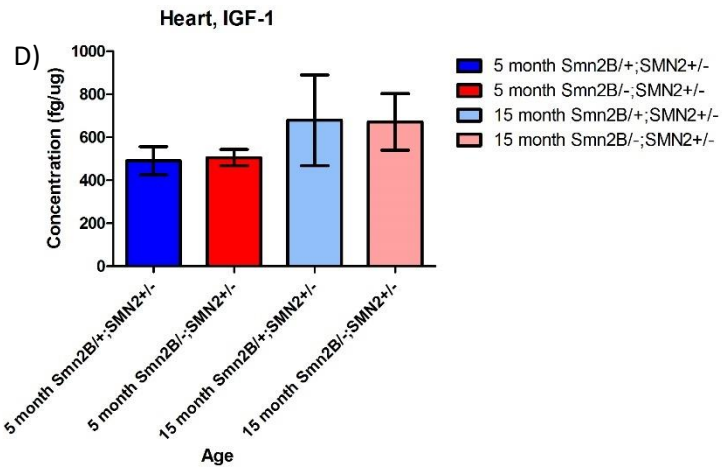
Heart, IGF-1
Concentration (fg/ug)
1000
800
600
400
200
0
5 month Smn2B/+;SMN2+/-
5 month Smn2B/-;SMN2+/-
15 month Smn2B/+;SMN2+/-
15 month Smn2B/-;SMN2+/-
Age

E)

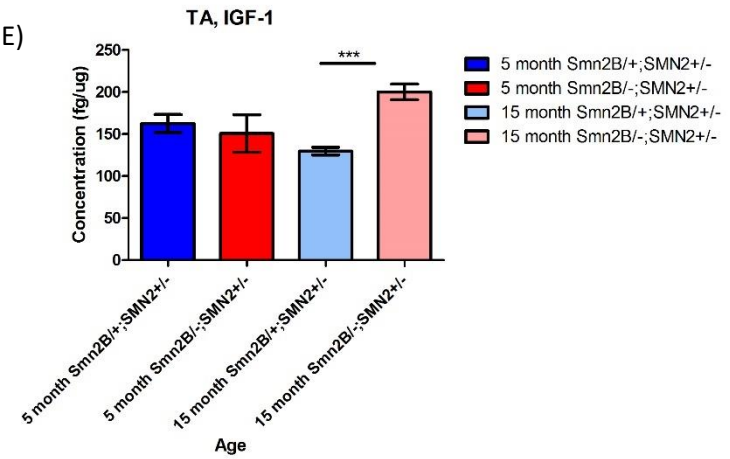
TA, IGF-1
Concentration (fg/ug)
250
200
150
100
50
0
***
5 month Smn2B/+;SMN2+/-
5 month Smn2B/-;SMN2+/-
15 month Smn2B/+;SMN2+/-
15 month Smn2B/-;SMN2+/-
Age

Figure 12. Mature IGF-1 protein product is increased within symptomatic stage *Smn$^{2B/-}$; SMN2$^{+/-}$* mouse TA muscle. ELISA displayed a significant IGF-1 increase within symptomatic TA muscle (E). No changes were observed in brain (A), SC (B), or heart (D) tissues as compared to *Smn$^{2B/+}$; SMN2$^{+/-}$* littermate controls. A mild decrease in IGF-1 however was observed in pre-symptomatic livers (C). Values were normalized to total protein added per well and represent mean ± SEM, n= 5, unpaired t test. *=p<0.05, **=p<0.01, ***=p<0.001, ****=p<0.0001.

3.4 *Trp53* mRNA is substantially increased in tibialis anterior muscle of symptomatic *Smn*$^{2B/-}$ mice, accompanied by an increase in downstream factors involved in p53 mediated apoptosis

In addition to our IGF-1 study, we wanted to determine if *Trp53* and subsequent p53 mediated apoptosis was occurring in the mouse models of SMA. Firstly, we examined *Trp53* mRNA levels in the *Smn*$^{2B/-}$ mice. We utilized the same tissues and qPCR protocol from previous studies (CNS, liver, heart, and TA muscle), and normalized values to *ActB* as an internal control.

We observed an increase in *Trp53* mRNA in pre-symptomatic spinal cords, symptomatic liver, and symptomatic TA skeletal muscle (Figure 12B, C, and D). The absence of a reliable and specific phospho-p53 antibody made measurements of p53 protein levels difficult. However, given the substantial upregulation of *Trp53* in the TA muscle, we decided to investigate both upstream p53 regulators and downstream factors to assess p53 mediated apoptosis.

A)

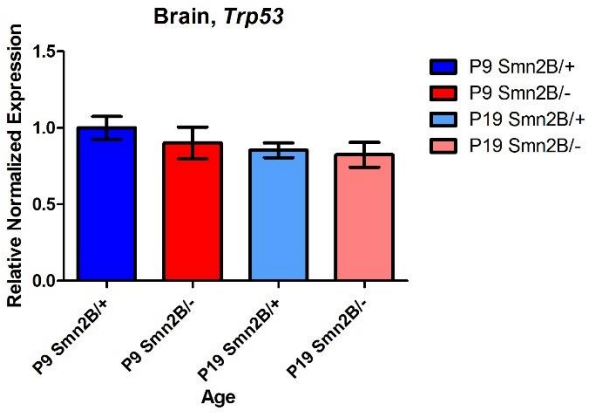
Brain, Trp53
Relative Normalized Expression
1.5
1.0
0.5
0.0
P9 Smn2B/+
P9 Smn2B/-
P19 Smn2B/+
P19 Smn2B/-
Age
P9 Smn2B/+
P9 Smn2B/-
P19 Smn2B/+
P19 Smn2B/-

B)

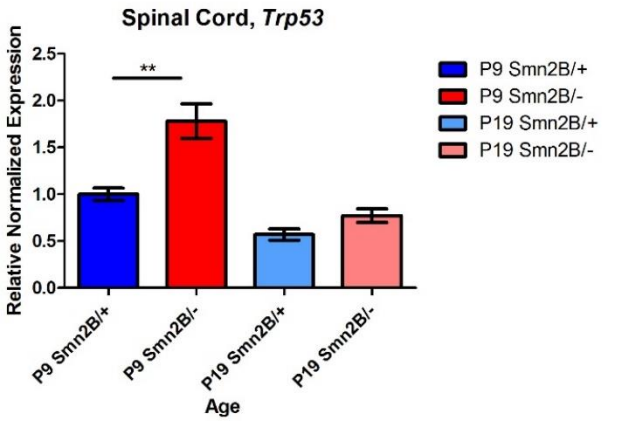
Spinal Cord, Trp53
Relative Normalized Expression
2.5
2.0
1.5
1.0
0.5
0.0
**
P9 Smn2B/+
P9 Smn2B/-
P19 Smn2B/+
P19 Smn2B/-
Age
P9 Smn2B/+
P9 Smn2B/-
P19 Smn2B/+
P19 Smn2B/-

C)

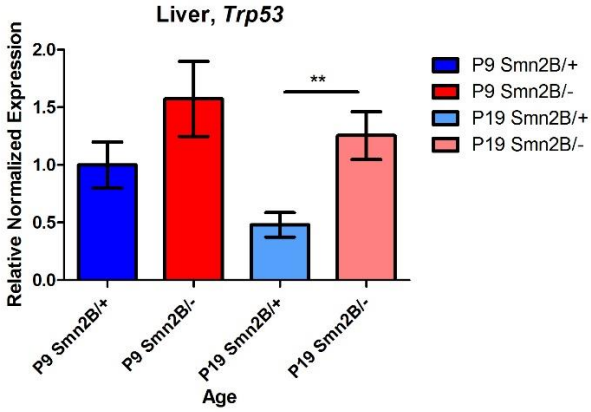
Liver, Trp53
Relative Normalized Expression
2.0
1.5
1.0
0.5
0.0
**
P9 Smn2B/+
P9 Smn2B/-
P19 Smn2B/+
P19 Smn2B/-
Age
P9 Smn2B/+
P9 Smn2B/-
P19 Smn2B/+
P19 Smn2B/-

D)

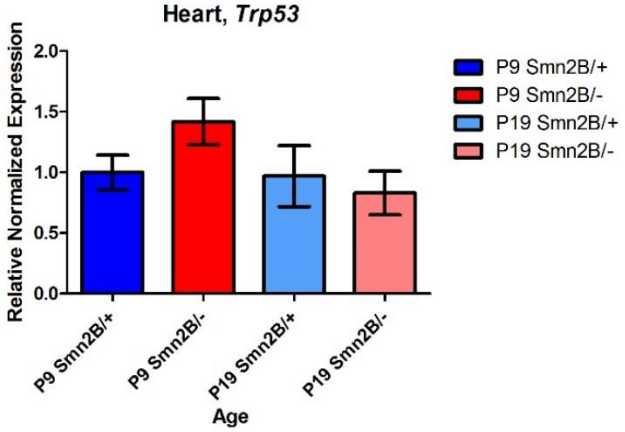
Heart, Trp53
Relative Normalized Expression
2.0
1.5
1.0
0.5
0.0
P9 Smn2B/+
P9 Smn2B/-
P19 Smn2B/+
P19 Smn2B/-
Age
P9 Smn2B/+
P9 Smn2B/-
P19 Smn2B/+
P19 Smn2B/-

E)

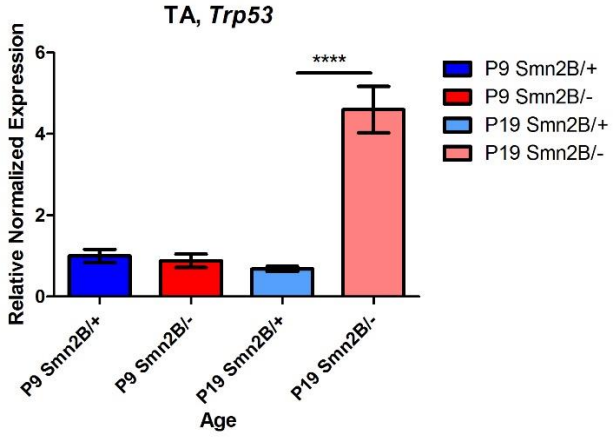
TA, Trp53
Relative Normalized Expression
6
4
2
0
****
P9 Smn2B/+
P9 Smn2B/-
P19 Smn2B/+
P19 Smn2B/-
Age
P9 Smn2B/+
P9 Smn2B/-
P19 Smn2B/+
P19 Smn2B/-

Figure 13. *Trp53* mRNA levels are significantly increased within pre-symptomatic SC, symptomatic livers, and symptomatic TA muscle of *Smn*$^{2B/-}$ mice. RT-qPCR analysis compared relative *Trp53* mRNA levels within brain (A), SC (B), liver (C), heart (D), and TA muscle (E) throughout disease course and compared to *Smn*$^{2B/+}$ littermate controls. Values were normalized to *ActB* expression and represent mean ± SEM, n = 3-6, unpaired t test. *=p<0.05, **=p<0.01, ***=p<0.001, ****=p<0.0001.

Within the TA muscle, we began by quantifying upstream factors known to regulate p53. Utilizing our RT-qPCR methods, *Cdkn1a* (encoding p21) and *Mdm2* (encoding Mdm2) mRNA expression was measured and normalized to *ActB* expression. These factors work to arrest cell cycle (p21) and ubiquitinate/repress p53 activity (mdm2 via negative feedback loop).

We observed that within symptomatic *Smn*$^{2B/-}$ TA muscle, both *Cdkn1a* (Figure 13A) and *Mdm2* (Figure 13B) mRNA expression was upregulated compared to their heterozygous littermates. Ultimately, an upregulation of these two factors at the protein level would influence p53 by arresting the cell cycle (allowing apoptosis or repair) and recreating the negative feedback loop to return p53 to baseline levels.

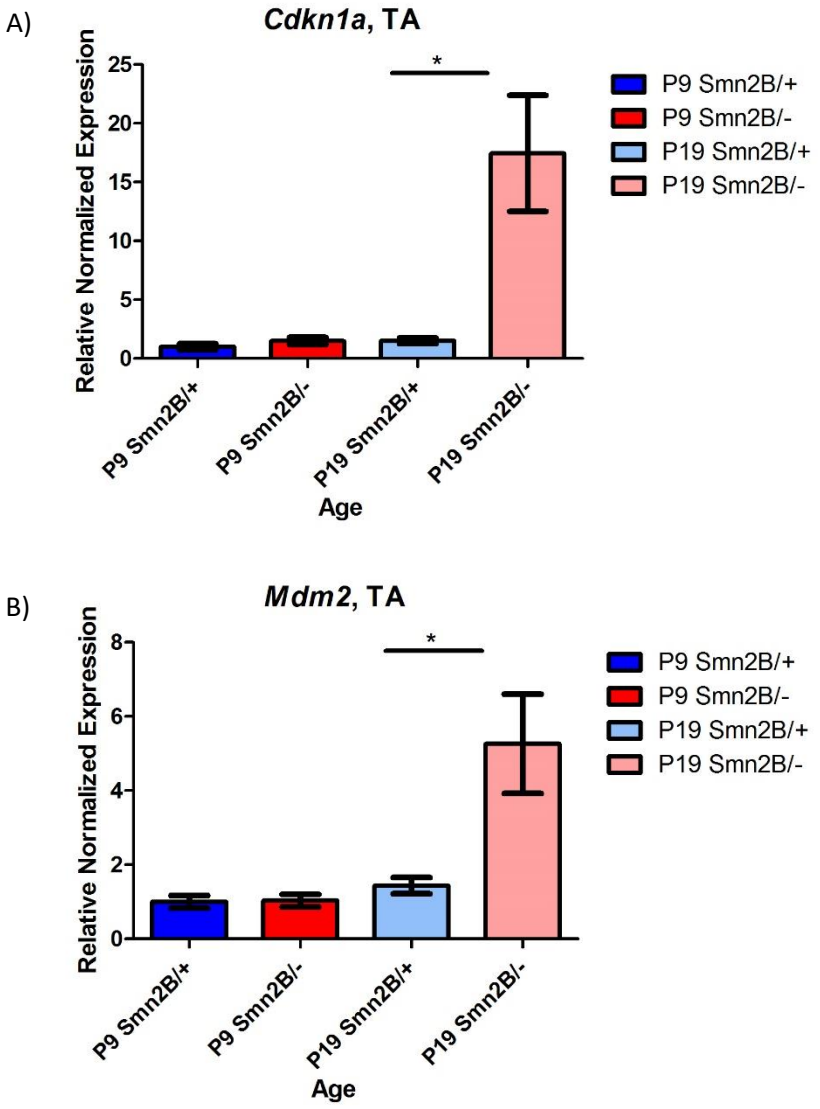

Figure 14. Upstream regulators of p53 are upregulated at the mRNA level within symptomatic *Smn*$^{2B/-}$ TA muscle. RT-qPCR analysis compared relative *Cdkn1a* (A) and *Mdm2* (B) expression levels within TA muscle throughout disease course and compared to *Smn*$^{2B/+}$ littermate controls. Values were normalized to *ActB* expression and represent mean ± SEM, n = 3-4, unpaired t test. *=p<0.05, **=p<0.01, ***=p<0.001, ****=p<0.0001.

Next, we examined the mRNA expression levels of several downstream factors known to play a role in p53 mediated apoptosis. *Pmaip1* and *Bbc3* for example, encoding Noxa and Puma proteins respectively, induce apoptosis through altering the mitochondrial outer membrane ultimately leading to the stimulation of caspases required to complete apoptosis. These among other BH3-Only proteins, are essential in p53 mediated apoptosis. We observed that within symptomatic TA muscle, all these downstream factors were upregulated (Figure 14).

A)

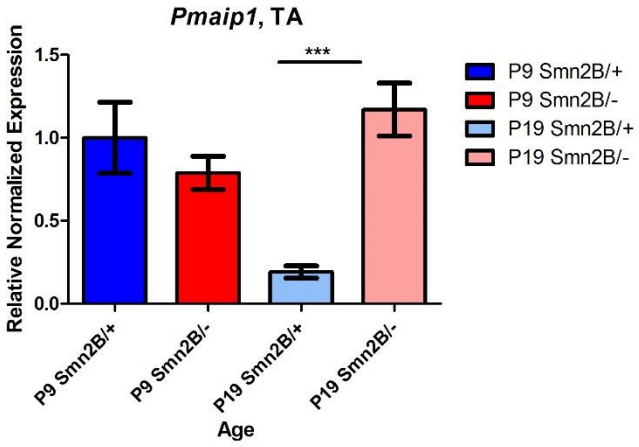
Pmaip1, TA
Relative Normalized Expression
1.5
1.0
0.5
0.0
***
P9 Smn2B/+
P9 Smn2B/-
P19 Smn2B/+
P19 Smn2B/-
P9 Smn2B/+
P9 Smn2B/-
P19 Smn2B/+
P19 Smn2B/-
Age

B)

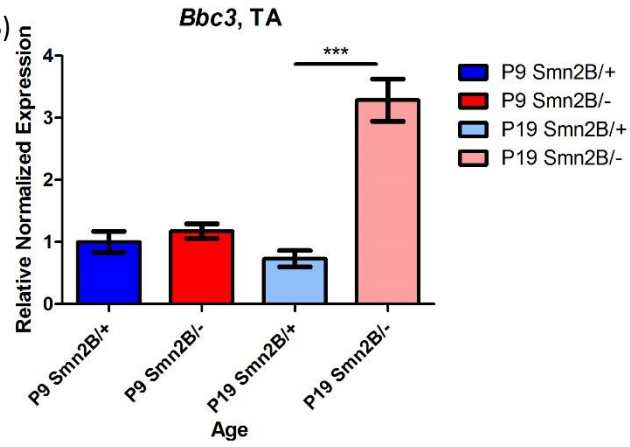
Bbc3, TA
Relative Normalized Expression
4
3
2
1
0
***
P9 Smn2B/+
P9 Smn2B/-
P19 Smn2B/+
P19 Smn2B/-
P9 Smn2B/+
P9 Smn2B/-
P19 Smn2B/+
P19 Smn2B/-
Age

C)

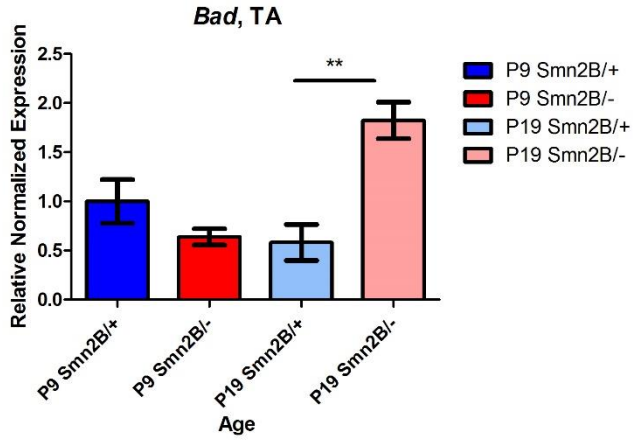
Bad, TA
Relative Normalized Expression
2.5
2.0
1.5
1.0
0.5
0.0
**
P9 Smn2B/+
P9 Smn2B/-
P19 Smn2B/+
P19 Smn2B/-
P9 Smn2B/+
P9 Smn2B/-
P19 Smn2B/+
P19 Smn2B/-
Age

D)

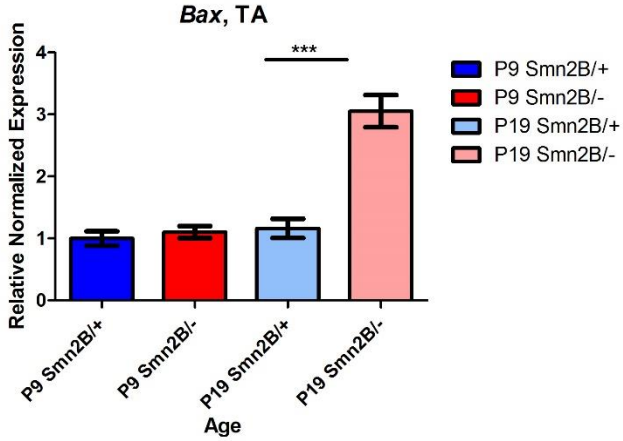
Bax, TA
Relative Normalized Expression
4
3
2
1
0
***
P9 Smn2B/+
P9 Smn2B/-
P19 Smn2B/+
P19 Smn2B/-
P9 Smn2B/+
P9 Smn2B/-
P19 Smn2B/+
P19 Smn2B/-
Age

E)

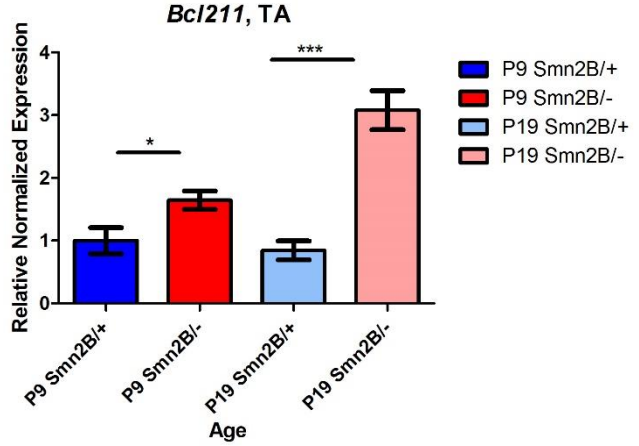
Bcl211, TA
Relative Normalized Expression
4
3
2
1
0
*
***
P9 Smn2B/+
P9 Smn2B/-
P19 Smn2B/+
P19 Smn2B/-
P9 Smn2B/+
P9 Smn2B/-
P19 Smn2B/+
P19 Smn2B/-
Age

Figure 15. Downstream apoptosis factors are upregulated at the mRNA level within symptomatic TA muscle of *Smn*$^{2B/-}$ mice. RT-qPCR analysis compared relative *Pmaip1* (A), *Bbc3* (B) *Bad* (C), *Bax* (D), and *Bcl-2l1* (E) expression levels within TA muscle throughout disease course and compared to *Smn*$^{2B/+}$ littermate controls. Values were normalized to *ActB* expression and represent mean ± SEM, n = 3-4, unpaired t test. *=p<0.05, **=p<0.01, ***=p<0.001, ****=p<0.0001.

3.5 *Trp53* mRNA and downstream pro-apoptotic factors are unchanged in the symptomatic tibialis anterior muscle of *Smn$^{2B/-}$; SMN2$^{+/-}$* mice

Finally, we investigated if *Trp53* expression is affected in the *Smn$^{2B/-}$; SMN2$^{+/-}$* model of mild SMA. Specifically, this would study the relationship between degree of SMN depletion and the degree of *Trp53* changes. To begin, CNS, liver, heart, and TA muscle were collected at pre-symptomatic (5 month) and symptomatic (15 month) timepoints and subjected to RNA extraction and RT-qPCR analysis.

Within the mild model, *Trp53* expression showed minimal dysregulation throughout disease course. Only the symptomatic stage TA muscle demonstrated a slight upregulation of *Trp53* at the mRNA level (Figure 15E). This provides a stark contrast to the upregulation of *Trp53* in multiple tissues within the *Smn$^{2B/-}$* model previously discussed.

We also measured the upstream factors involved in the regulation of p53, as well as downstream pro-apoptotic factors at the mRNA level. *Cdkn1a* and *Mdm2* expression was recorded and normalized to *ActB* expression via RT-qPCR analysis at 5- and 15-month timepoints. Interestingly, *Cdkn1a* mRNA was upregulated at both timepoints in the TA muscle (Figure 16A). When downstream pro-apoptosis factors were examined, only *Bcl2* was mildly upregulated in symptomatic TA muscle (Figure 17C). Overall, the *Smn$^{2B/-}$; SMN2$^{+/-}$* model of mild SMA demonstrated no strong signs of p53 mediated apoptosis, as opposed to the *Smn$^{2B/-}$* model, within TA skeletal muscle.

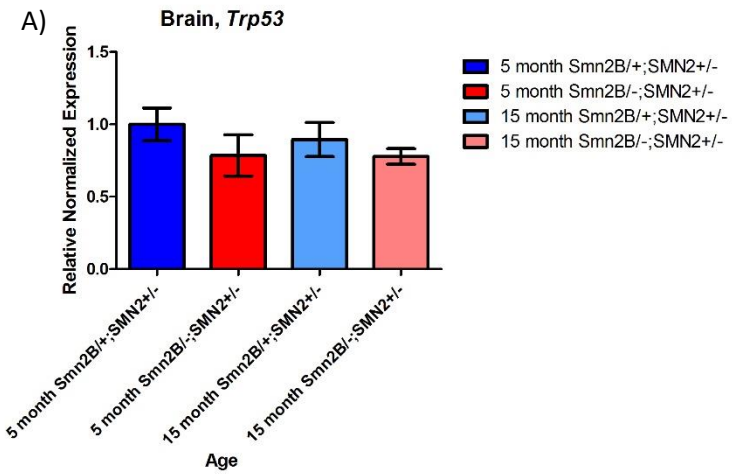
A)
Brain, Trp53
Relative Normalized Expression
1.5
1.0
0.5
0.0
5 month Smn2B/+;SMN2+/-
5 month Smn2B/-;SMN2+/-
15 month Smn2B/+;SMN2+/-
15 month Smn2B/-;SMN2+/-
Age

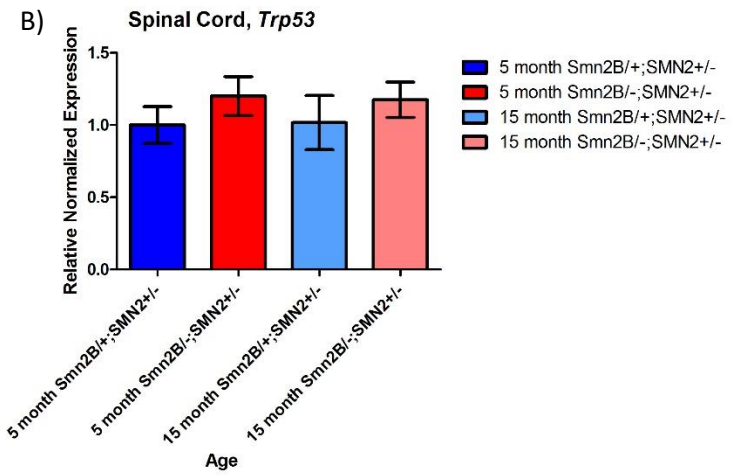
B)
Spinal Cord, Trp53
Relative Normalized Expression
1.5
1.0
0.5
0.0
5 month Smn2B/+;SMN2+/-
5 month Smn2B/-;SMN2+/-
15 month Smn2B/+;SMN2+/-
15 month Smn2B/-;SMN2+/-
Age

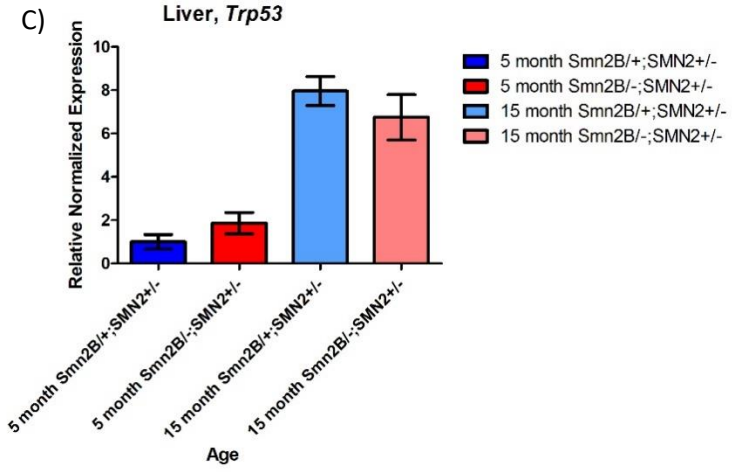
C)
Liver, Trp53
Relative Normalized Expression
10
8
6
4
2
0
5 month Smn2B/+;SMN2+/-
5 month Smn2B/-;SMN2+/-
15 month Smn2B/+;SMN2+/-
15 month Smn2B/-;SMN2+/-
Age

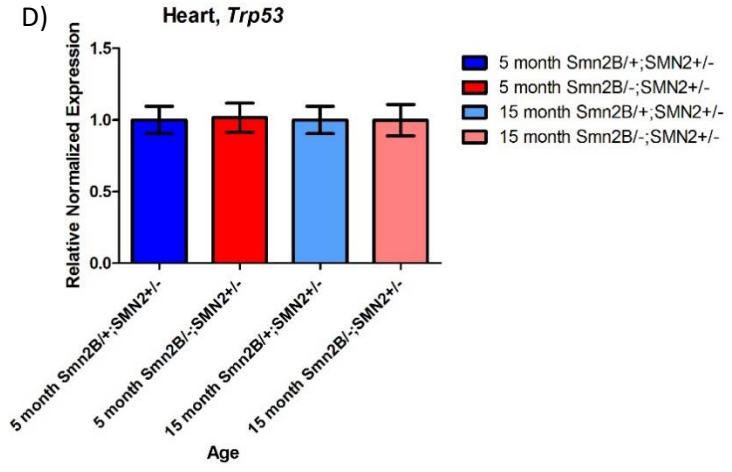
D)
Heart, Trp53
Relative Normalized Expression
1.5
1.0
0.5
0.0
5 month Smn2B/+;SMN2+/-
5 month Smn2B/-;SMN2+/-
15 month Smn2B/+;SMN2+/-
15 month Smn2B/-;SMN2+/-
Age

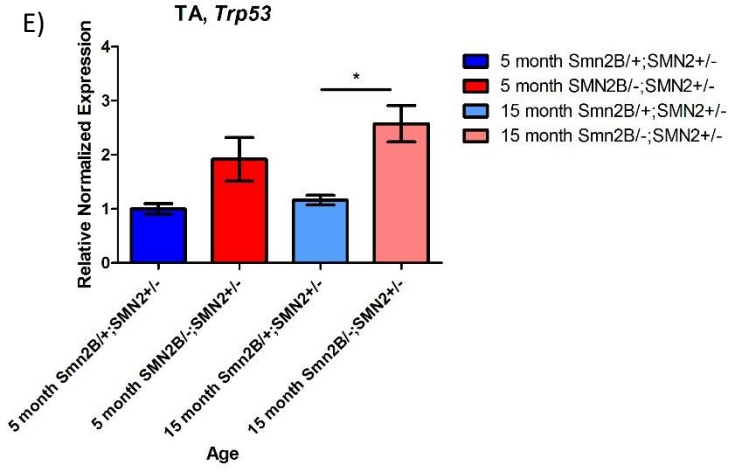
E)
TA, Trp53
Relative Normalized Expression
4
3
2
1
0
*
5 month Smn2B/+;SMN2+/-
5 month SMN2B/-;SMN2+/-
15 month Smn2B/+;SMN2+/-
15 month Smn2B/-;SMN2+/-
Age

Figure 16. *Trp53* mRNA levels are slightly increased within symptomatic *Smn$^{2B/-}$; SMN2$^{+/-}$* TA muscle. RT-qPCR analysis compared relative *Trp53* expression levels within brain (A), SC (B), liver (C), heart (D), and TA muscle (E) throughout disease course and compared to *Smn$^{2B/+}$; SMN2$^{+/-}$* littermate controls. Values were normalized to *ActB* expression and represent mean ± SEM, n = 5, unpaired t test. *=p<0.05, **=p<0.01, ***=p<0.001, ****=p<0.0001.

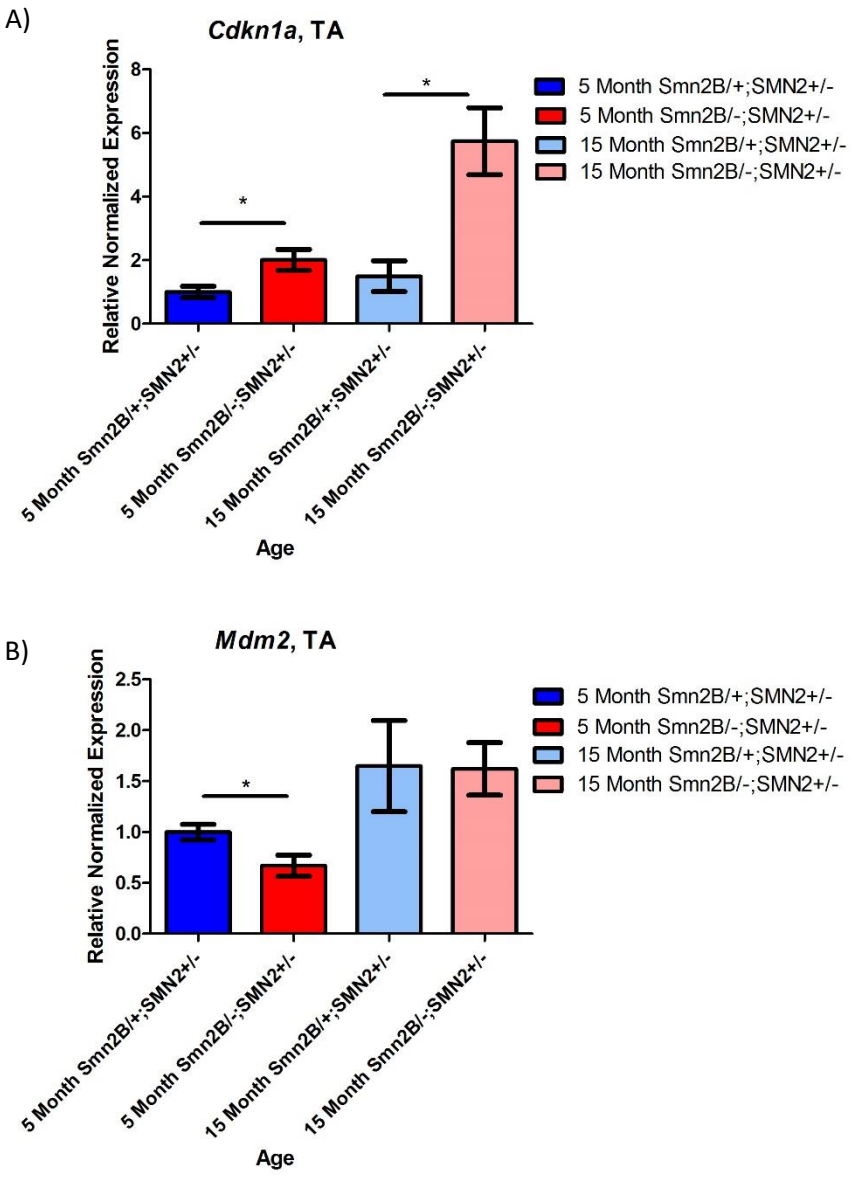

Figure 17. Factors involved in cell cycle arrest are upregulated at the mRNA level within both pre-symptomatic and symptomatic *Smn$^{2B/-}$; SMN2$^{+/-}$* TA muscle. RT-qPCR analysis compared relative *Cdkn1a* (A) and *Mdm2* (B) expression levels within TA muscle throughout disease course and compared to *Smn$^{2B/+}$; SMN2$^{+/-}$* littermate controls. Values were normalized to *ActB* expression and represent mean ± SEM, n = 3-4, unpaired t test. *=p<0.05, **=p<0.01, ***=p<0.001, ****=p<0.0001.

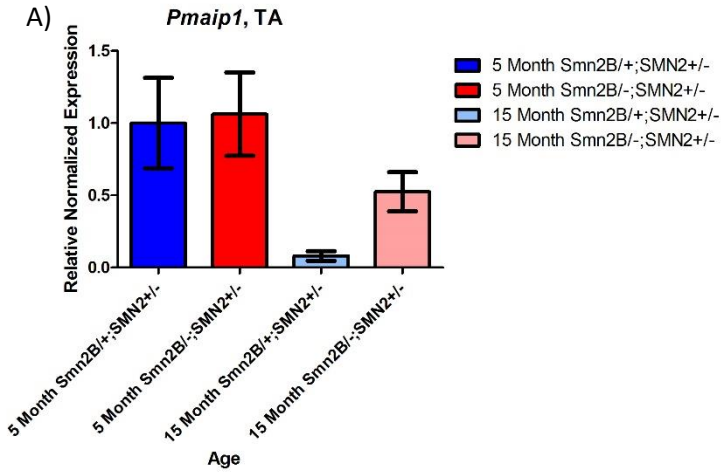
A)
Pmaip1, TA
Relative Normalized Expression
1.5
1.0
0.5
0.0
5 Month Smn2B/+;SMN2+/-
5 Month Smn2B/-;SMN2+/-
15 Month Smn2B/+;SMN2+/-
15 Month Smn2B/-;SMN2+/-
5 Month Smn2B/+;SMN2+/-
5 Month Smn2B/-;SMN2+/-
15 Month Smn2B/+;SMN2+/-
15 Month Smn2B/-;SMN2+/-
Age

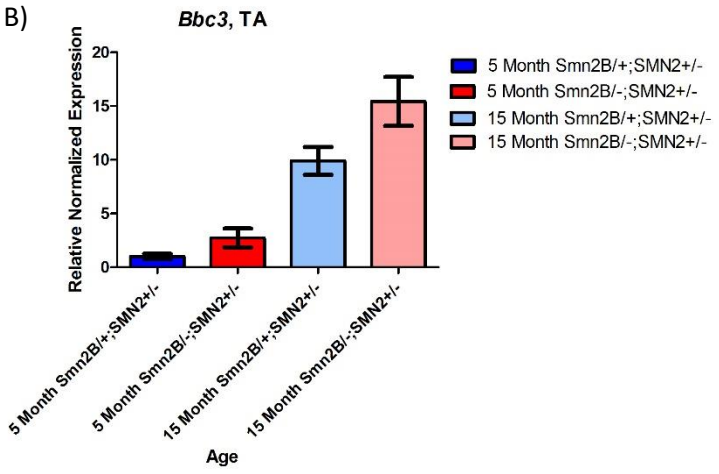
B)
Bbc3, TA
Relative Normalized Expression
20
15
10
5
0
5 Month Smn2B/+;SMN2+/-
5 Month Smn2B/-;SMN2+/-
15 Month Smn2B/+;SMN2+/-
15 Month Smn2B/-;SMN2+/-
5 Month Smn2B/+;SMN2+/-
5 Month Smn2B/-;SMN2+/-
15 Month Smn2B/+;SMN2+/-
15 Month Smn2B/-;SMN2+/-
Age

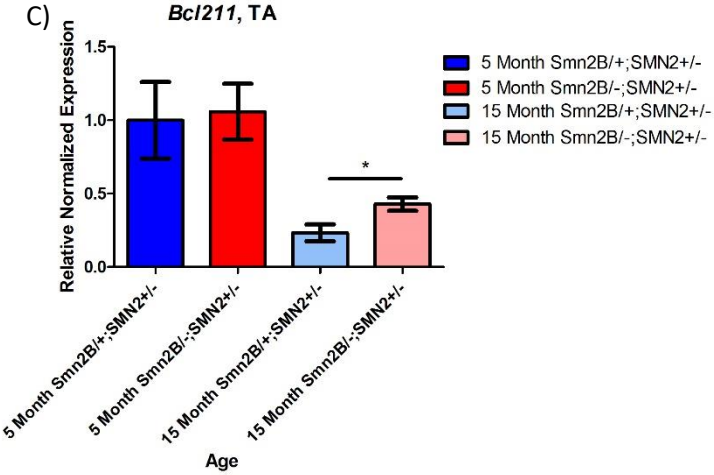
C)
Bcl211, TA
Relative Normalized Expression
1.5
1.0
0.5
0.0
*
5 Month Smn2B/+;SMN2+/-
5 Month Smn2B/-;SMN2+/-
15 Month Smn2B/+;SMN2+/-
15 Month Smn2B/-;SMN2+/-
5 Month Smn2B/+;SMN2+/-
5 Month Smn2B/-;SMN2+/-
15 Month Smn2B/+;SMN2+/-
15 Month Smn2B/-;SMN2+/-
Age

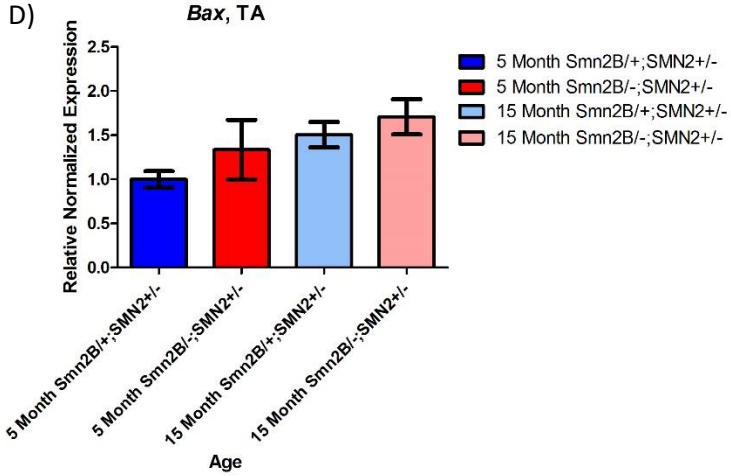
D)
Bax, TA
Relative Normalized Expression
2.5
2.0
1.5
1.0
0.5
0.0
5 Month Smn2B/+;SMN2+/-
5 Month Smn2B/-;SMN2+/-
15 Month Smn2B/+;SMN2+/-
15 Month Smn2B/-;SMN2+/-
5 Month Smn2B/+;SMN2+/-
5 Month Smn2B/-;SMN2+/-
15 Month Smn2B/+;SMN2+/-
15 Month Smn2B/-;SMN2+/-
Age

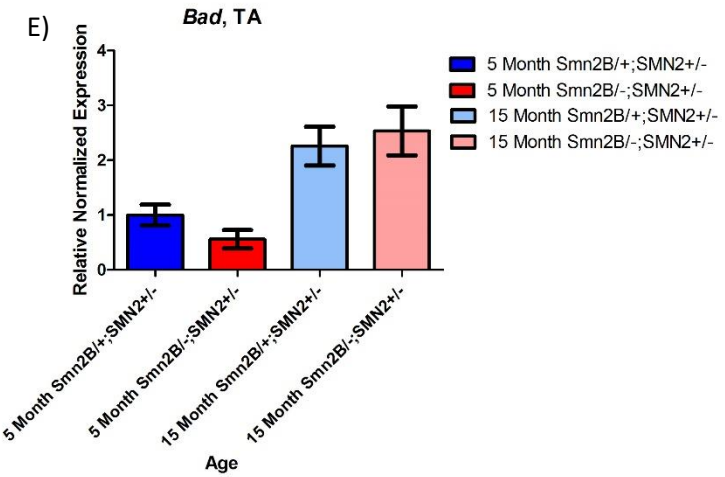
E)
Bad, TA
Relative Normalized Expression
4
3
2
1
0
5 Month Smn2B/+;SMN2+/-
5 Month Smn2B/-;SMN2+/-
15 Month Smn2B/+;SMN2+/-
15 Month Smn2B/-;SMN2+/-
5 Month Smn2B/+;SMN2+/-
5 Month Smn2B/-;SMN2+/-
15 Month Smn2B/+;SMN2+/-
15 Month Smn2B/-;SMN2+/-
Age

Figure 18. Factors involved in p53 mediated apoptosis remain unchanged at the mRNA level within TA muscle of the *Smn$^{2B/-}$; SMN2$^{+/-}$* mice. RT-qPCR analysis compared relative *Pmaip1* (A), *Bbc3* (B) *Bcl-2l1* (C), *Bax* (D), and *Bad* (E) expression levels within TA muscle throughout disease course and compared to *Smn$^{2B/+}$; SMN2$^{+/-}$* littermate controls. Values were normalized to *ActB* expression and represent mean ± SEM, n = 3-4, unpaired t test. *=p<0.05, **=p<0.01, ***=p<0.001, ****=p<0.0001.

4. Discussion

SMA is a critical neurodegenerative condition whose phenotype depends on the degree of SMN protein depletion in the body. In severe cases, levels of circulating FL-SMN are insufficiently low, resulting in a wide range of symptomology not confined to CNS tissues. In mild cases, SMN levels remain insufficient to prevent disease, however a pathogenic phenotype is attenuated dramatically. Our laboratory has generated two mouse models of SMA which highlight these varying phenotypes because of different degrees of SMN depletion.

4.1 SMN protein is decreased in both severe and mild mouse models of SMA

Previous work in our laboratory has developed and validated two mouse models of SMA which represent the varying phenotypes observed in the patient population. The *Smn*$^{2B/-}$ model represents a severe phenotype including MN death, NMJ pathology, NAFLD, muscle wasting, and premature death.[11] However by adding an additional human *SMN2* transgene within the mutant background, one can increase levels of FL-SMN and generate a mild model of SMA.[12] This effectively improves lifespan, degree of MN and NMJ pathology, and extra-neuronal pathology.

Our study outlined the SMN levels in both models throughout disease course in the CNS and in peripheral tissues. We validated that within *Smn*$^{2B/-}$ mice, SMN protein is significantly decreased in brain, SC, liver, heart, and TA skeletal muscle at all timepoints (Figure 4 and 5) as compared to their normal heterozygous littermates. In addition, the *Smn*$^{2B/-}$*; SMN2*$^{+/-}$ model of mild SMA also displays decreased levels of SMN in the CNS and periphery (Figure 6 and 7). This decrease however is less than the depletion observed within the severe mice. These models therefore represent the consequences of varying levels of SMN depletion. We utilized this to

outline downstream effects of varying SMN depletion in the two different mouse models of SMA.

4.2 *Igf-1* is reduced in the severe model of SMA, resulting in widespread deficiency in the peripheral tissues

Igf-1 mRNA is decreased within symptomatic $Smn^{2B/-}$ livers (Figure 8C). Since the liver serves as one of the primary IGF-1 protein production sites, it is perhaps unsurprising that consequently IGF-1 protein is decreased within all peripheral tissues tested in the severe model (Figure 9C-E). Interestingly, within the $Smn^{2B/-}$; $SMN2^{+/-}$ model where the SMN depletion is not as severe, we observe an attenuation of the changes in IGF-1. Indeed, *Igf-1* mRNA levels were mildly increased within SMA effected livers, resulting in increased IGF-1 protein in the TA muscle mice at the symptomatic timepoint.

It is interesting to note the differences between models regarding motor function and muscle pathology at this symptomatic stage. For example, $Smn^{2B/-}$ mice experience substantial muscle atrophy, decreased muscle fibre size, MN loss and impaired mobility at their symptomatic timepoint while $Smn^{2B/-}$; $SMN2^{+/-}$ mice experience only mild but sustained motor weakness and atrophy. Given the role of IGF-1 in protein synthesis and muscle growth, this depletion in the $Smn^{2B/-}$ mice highlight a potential mechanism contributing to muscle defects as well as overall growth impairment. For instance, a systemic reintroduction of IGF-1 protein in $Smn^{2B/-}$ mice via viral vector could be therapeutically useful in the context of severe SMA.

This current evidence that our laboratory provides in support of IGF-1 changes within SMA is further complimented by the literature. As previously discussed, multiple studies have demonstrated decreased levels of IGF-1 in the context of SMA. For example, IGF-1 is decreased

in both SMA patient as well as *Smn*$^{2B/-}$ mouse model serum.[24,38] Overall, our investigation furthers the evidence supporting SMN dependant IGF-1 defects in severe models of SMA.

4.3 Therapeutic potential of IGF-1 as a SMN independent therapy

To date, IGF-1 replacement therapies are commonly used in practice to treat conditions which produce IGF-1 deficiencies. For instance, Laron Syndrome, liver cirrhosis, metabolic syndrome, neurodegenerative disorders (AD and ALS), and age-related loss of muscle density may all be treated with supplemental IGF-1.[57] These therapies work by exploiting IGF-1's role in protein synthesis, muscle growth, neuroprotective properties, and proliferative properties to improve quality of life. Currently, recombinant human IGF-1 (rhIGF-1) is an FDA approved option given to patients with primary IGF-1 deficiency.

Given these neuroprotective and muscle building aspects of supplemental rhIGF-1, this treatment proposes an intriguing option for current SMA patients. Current literature has outlined the benefits of systemically increasing IGF-1. For example, by administering IPLEX (combination of hIGF-1 and rhIGFBP-3) in *SMNΔ7* mice, motor functions and MN loss improved.[38] Similarly, when IGF-1 was overexpressed systemically in these mice, improvements were seen in motor coordination.[43] Given the time-sensitive aspect of treating SMA, supplemental IGF-1 presents as a novel SMN-independent therapeutic.

Overall, we have demonstrated that our *Smn*$^{2B/-}$ model mice in particular show widespread IGF-1 defects throughout the periphery (Figures 8 and 9). The phenotype reflects the decreased body weight, delay in growth, muscle wasting, and motor impairments that coincides with severe subtypes of the SMA patient population. Given IGF-1's role in neuroprotection, growth, and protein synthesis it is now proposed that IGF-1 treatments be investigated in this model.

4.4 Evidence for p53 mediated apoptosis within SMA skeletal muscle tissue as a result of severe SMN depletion

Within the *Smn*$^{2B/-}$ model of severe SMA, an upregulation of *Trp53* at the mRNA level was observed in multiple tissues (Figure 12). The most substantial upregulation however proved to be in the TA skeletal muscle of symptomatic *Smn*$^{2B/-}$ mice. Upon further investigation of this tissue, it was observed that there was also an upregulation of *Mdm2* and *Cdkn1a* (Figure 13) mRNA expression. Increased *Mdm2* may indicate the workings of the negative feedback loop involved in returning p53 levels to baseline levels. Interestingly, increased *Cdkn1a* may indicate the arrest of the cell cycle through p21 binding/halting the CDK/Cyclin complex. Additionally, the increase in BH3-Only mRNA transcripts (Figure 14) suggests the occurrence of p53 mediated apoptosis in TA muscle. The over-expression of pro-apoptotic factors (BH3-Only protein transcripts) would then work to inhibit the lesser amounts of *Bcl-2* anti-apoptotic factor (Figure 18A). Interestingly, within the mild model of SMA, the levels of BH3-Only protein transcripts remain unchanged while transcripts encoding the anti-apoptotic *Bcl-2* are elevated. Alongside this, *Cdkn1a* remains elevated suggesting cell cycle arrest. Overall, this shift in the balance between pro vs anti-apoptotic factors shifts the scales to favor cell survival (Figure 18B).

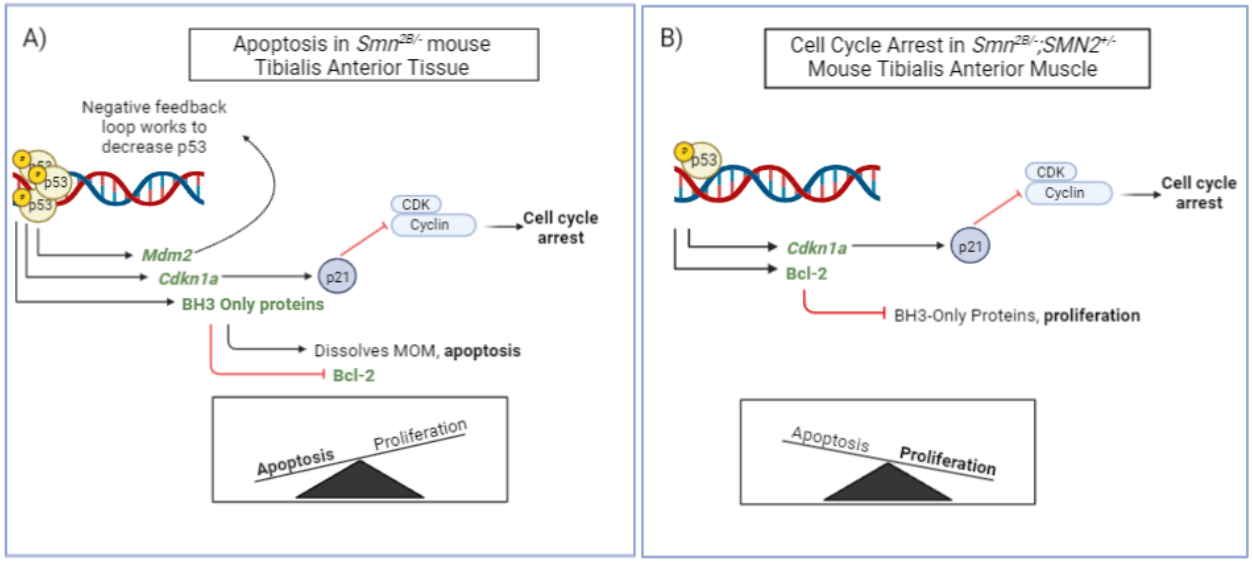

Figure 19. Illustrated summary of *Trp53* pathways in severe vs mild mouse models of SMA within Tibialis Anterior skeletal muscle. A) Severe model mice have high mRNA levels of *Cdkn1a*, and pro-apoptotic BH3-Only protein mRNA resulting in apoptosis. B) Mild model mice display mRNA expression of *Cdkn1a* suggesting cell cycle arrest, however more expression of anti-apoptotic Bcl-2 than BH3-only family mRNA resulting in survival. Created by BioRender.

An increase in *Trp53* at both the mRNA and protein levels has previously been documented within the context of SMA. However, most reports in the literature focus on the increase of p53 in SMA effected MNs. Interestingly, one study highlighted the finding of early muscle cell death within the Taiwanese model of severe SMA.[58] Their primary conclusion stated that faulty DNA repair in muscle tissues resulting from insufficient SMN could contribute to its cellular death. Although they were not able to detect upregulation of p-p53, p53 was found to be increased at early stages of the disease.[58] Overall, this muscle damage preceded DNA damage in MNs within this model. A postnatal p53 reduction in the *Smn*$^{2B/-}$ model of SMA provided additional evidence for the loss of NMJs before MNs.[54] In more detail, researchers determined that p53 related transcripts were upregulated in the cell body at the onset of NMJ pathology.

Given this, p53 was then selectively knocked out at a presymptomatic timepoint to determine its possible role in NMJ pathology. It was ultimately found that when p53 was reduced, loss of NMJs were attenuated while MN pathology remained, suggesting NMJ loss is p53-dependant in the *Smn*$^{2B/-}$ model of SMA.[54] Interestingly, another model of p53 muscle-specific knock out examined elements of the mitochondrial quality control (MQC) pathways after denervation stress. p53 KO specifically in muscle exacerbated the dysregulation of MQC pathways after denervation, suggesting that p53 regulates MQC in the event of muscle atrophy.[59] Overall, p53's role in the skeletal muscle of SMA effected individuals remains under characterized. More investigation is required to fully understand its relationship to SMN in the context of SMA.

Furthermore, the IGF-1/p53 relationship also remains particularly interesting in the context of this study. It has been previously determined that wild type p53 can regulate the entirety of the IGF-1 axis through the control of ligand, receptor, and IGF1BP expression. These two pathways with opposing goals (growth versus destruction) converge to regulate cell fate. For example, within the TA tissue of mild *Smn*$^{2B/-}$*; SMN2*$^{+/-}$ mice, IGF-1 was increased while *Trp53* and downstream apoptosis factors were relatively unchanged. In essence, the stimulation of the IGF-1 growth pathway would lead to the increased levels of Akt protein kinase and mTOR. These have been established to inhibit p53 accumulation in a Mdm2 dependant manner (Figure 19A). This would result in protein synthesis and cellular growth/maintenance to occur within the TA tissue of mild SMA mice. In contrast, the severe *Smn*$^{2B/-}$ mice displayed decreased IGF-1 and increased transcripts for *Trp53* and downstream apoptosis factors. In the event of large enough damage, stress signals promote the phosphorylation and stabilization of p53. P-p53 is then capable to directly stimulate the production of IGF-1BPs and PTEN (which works to inhibit Pip2 phosphorylation (via PI3K) to ultimately halt the IGF-1 growth signalling axis in the event of

damage (Figure 19B). Accumulation of p-p53 may then lead to apoptosis or cellular arrest as previously described.

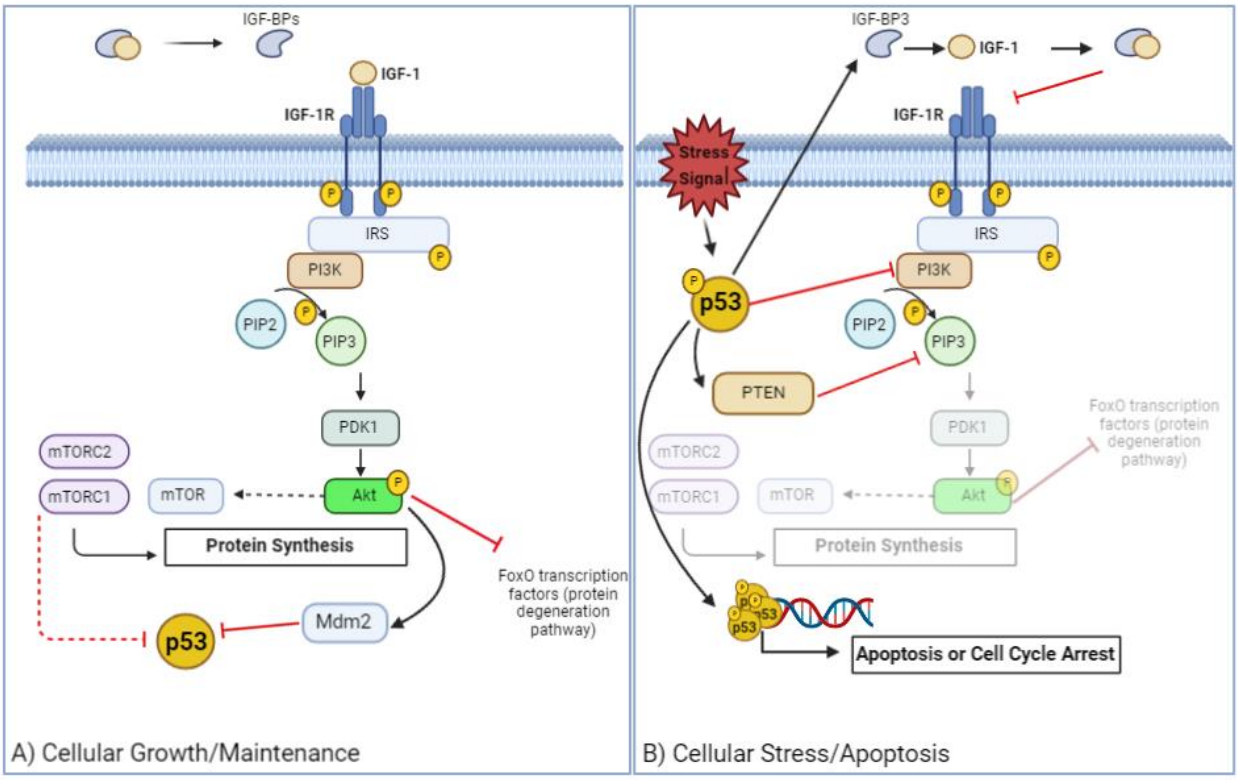

Figure 20. IGF-1/p53 relationship in cellular growth or destruction. A) IGF-1 participates in protein synthesis and growth through use of the Akt/mTOR pathway. Several of these components are also involved in the repression of p53 mediated destruction. B) In the event of cellular stress, p53 is phosphorylated and later represses factors involved in IGF-1 growth pathway either directly or indirectly. Created by BioRender.

In conclusion, our investigation provides evidence of p53 mediated apoptosis in severe, but not mild, SMN depletion. Severely ill mice displayed poor motor function alongside decreased IGF-1, elevated transcript levels of pro-apoptotic factors as contrasted by the mild model which experienced increased IGF-1 and upregulation of transcripts involved in cell cycle arrest and repair.

4.5 Future directions

Our study outlines widespread IGF-1 changes and evidence of p53 mediated apoptosis in the severe *Smn*$^{2B/-}$ model of SMA. These findings are attenuated in the *Smn*$^{2B/-}$*; SMN2*$^{+/-}$ model of mild SMA. To further understand the role IGF-1 plays in severe SMA, as well as its relationship to p53 in skeletal muscle, it is recommended that several studies be performed. Firstly, it is suggested that *Igf-1* variant isoforms are identified through RNA sequencing. Given SMN's role in splicing, the identification of *Igf-1* splice variants specific to SMN depletion could provide insight into the varying expression levels of IGF-1 in SMA effected individuals versus littermate controls. Furthermore, an investigation of p53 mediated apoptosis in severe SMA affected skeletal muscle should be continued. This could include quantifying p53, p-p53, and downstream apoptosis factors at the protein level via western blot or immunohistochemistry to further validate our transcript findings. Additionally, one could investigate muscle death within the context of SMN restorative or IGF-1 replacement therapies. For example, detection of p53 mediated apoptosis in TA muscle could be studied after the administration of rhIGF-1 which is already available to patients today. Additionally, effects of overall growth, survival, and motor coordination could be tested. Overall, the IGF-1/p53 relationship as well as each factor individually requires further investigation to outline cell death pathways in muscle tissue to increase support for SMN independent therapies for SMA.

5. Conclusion

In this investigation, we determined that the *Smn*$^{2B/-}$ and *Smn*$^{2B/-}$*; SMN2*$^{+/-}$ mouse models produce decreased levels of SMN protein representative of severe and mild SMA phenotypes respectively. As a consequence of SMN depletion, widespread IGF-1 downregulation in peripheral tissues and stark *Trp53* upregulation within TA muscle outline extra-neuronal defects in severe subtypes of SMA. We demonstrated that these defects are dependent on the degree of SMN depletion and attenuated in more mild cases of the disease. Additionally, observed changes in gene expression or protein quantification was tissue dependant. Altogether, our study highlights systemic IGF-1 defects which further investigation, as well as evidence for p53 mediated apoptosis within skeletal muscle tissue.

References

1. D'Amico, A., Mercuri, E., Tiziano, F. D. & Bertini, E. Spinal muscular atrophy. *Orphanet J. Rare Dis.* **6**, 1–10 (2011).

2. Kolb, S. J. & Kissel, J. T. Spinal Muscular Atrophy. *Neurol. Clin.* **33**, 831 (2015).

3. Prior, T. W. *et al.* Newborn and carrier screening for spinal muscular atrophy. *Am. J. Med. Genet. Part A* **152**, 1608–1616 (2010).

4. Singh, R. N., Howell, M. D., Ottesen, E. W. & Singh, N. N. Diverse role of Survival Motor Neuron Protein. *Biochim. Biophys. Acta* **1860**, 299 (2017).

5. Lefebvre, S. *et al.* Identification and characterization of a spinal muscular atrophy-determining gene. *Cell* **80**, 155–165 (1995).

6. Locatelli, D. *et al.* Human Axonal Survival of Motor Neuron (a-SMN) Protein Stimulates Axon Growth, Cell Motility, C-C Motif Ligand 2 (CCL2), and Insulin-like Growth Factor-1 (IGF1) Production. *J. Biol. Chem.* **287**, 25782 (2012).

7. Seo, J., Singh, N. N., Ottesen, E. W., Lee, B. M. & Singh, R. N. A novel human-specific splice isoform alters the critical C-terminus of Survival Motor Neuron protein. *Sci. Rep.* **6**, (2016).

8. Antoine, M. *et al.* Splicing Defects of the Profilin Gene Alter Actin Dynamics in an S. pombe SMN Mutant. *iScience* **23**, (2020).

9. Hsieh-Li, H. M. *et al.* A mouse model for spinal muscular atrophy. *Nat. Genet.* **24**, 66–71 (2000).

10. Le, T. T. *et al.* SMNΔ7, the major product of the centromeric survival motor neuron

(SMN2) gene, extends survival in mice with spinal muscular atrophy and associates with full-length SMN. *Hum. Mol. Genet.* **14**, 845–857 (2005).

11. Bowerman, M., Murray, L. M., Beauvais, A., Pinheiro, B. & Kothary, R. A critical smn threshold in mice dictates onset of an intermediate spinal muscular atrophy phenotype associated with a distinct neuromuscular junction pathology. *Neuromuscul. Disord.* **22**, 263–276 (2012).

12. Deguise, M. O. *et al.* Motor transmission defects with sex differences in a new mouse model of mild spinal muscular atrophy. *EBioMedicine* **55**, (2020).

13. Chaytow, H., Huang, Y. T., Gillingwater, T. H. & Faller, K. M. E. The role of survival motor neuron protein (SMN) in protein homeostasis. *Cellular and Molecular Life Sciences* **75**, 3877–3894 (2018).

14. Groen, E. J. N. *et al.* Temporal and tissue-specific variability of SMN protein levels in mouse models of spinal muscular atrophy. *Hum. Mol. Genet.* **27**, 2851–2862 (2018).

15. Zhao, X. *et al.* SMN protein is required throughout life to prevent spinal muscular atrophy disease progression. *Hum. Mol. Genet.* **31**, 82–96 (2021).

16. Zhang, H. L. *et al.* Active Transport of the Survival Motor Neuron Protein and the Role of Exon-7 in Cytoplasmic Localization. (2003).

17. Pletto, D. *et al.* Axon outgrowth and neuronal differentiation defects after a-SMN and FL-SMN silencing in primary hippocampal cultures. *PLoS One* **13**, e0199105–e0199105 (2018).

18. Laird, A. S., Mackovski, N., Rinkwitz, S., Becker, T. S. & Giacomotto, J. Tissue-specific

models of spinal muscular atrophy confirm a critical role of SMN in motor neurons from embryonic to adult stages. *Hum. Mol. Genet.* **25**, 1728–1738 (2016).

19. Besse, A. *et al.* AAV9-Mediated Expression of SMN Restricted to Neurons Does Not Rescue the Spinal Muscular Atrophy Phenotype in Mice. *Mol. Ther.* **28**, 1887–1901 (2020).

20. Wijngaarde, C. A. *et al.* Cardiac pathology in spinal muscular atrophy: a systematic review. *Orphanet J. Rare Dis.* **12**, 1–10 (2017).

21. Motyl, A. A. L. *et al.* Pre-natal manifestation of systemic developmental abnormalities in spinal muscular atrophy. *Hum. Mol. Genet.* **29**, 2674–2683 (2020).

22. Shababi, M. *et al.* Cardiac defects contribute to the pathology of spinal muscular atrophy models. *Hum. Mol. Genet.* **19**, 4059–4071 (2010).

23. Szunyogova, E. *et al.* Survival Motor Neuron (SMN) protein is required for normal mouse liver development. *Sci. Rep.* **6**, (2016).

24. Deguise, M. O. *et al.* SMN Depleted Mice Offer a Robust and Rapid Onset Model of Nonalcoholic Fatty Liver Disease. *Cell. Mol. Gastroenterol. Hepatol.* **12**, 354 (2021).

25. Deguise, M. O. *et al.* Abnormal fatty acid metabolism is a core component of spinal muscular atrophy. *Ann. Clin. Transl. Neurol.* **6**, 1519 (2019).

26. Ando, S. *et al.* SMN Protein Contributes to Skeletal Muscle Cell Maturation Via Caspase-3 and Akt Activation. *In Vivo (Brooklyn).* **34**, 3247 (2020).

27. Kim, J. K. *et al.* Muscle-specific SMN reduction reveals motor neuron–independent disease in spinal muscular atrophy models. *J. Clin. Invest.* **130**, 1271 (2020).

28. Goodkey, K., Aslesh, T., Maruyama, R. & Yokota, T. Nusinersen in the Treatment of Spinal Muscular Atrophy. *Methods Mol. Biol.* **1828**, 69–76 (2018).

29. Stevens, D., Claborn, M. K., Gildon, B. L., Kessler, T. L. & Walker, C. Onasemnogene Abeparvovec-xioi: Gene Therapy for Spinal Muscular Atrophy. *Ann. Pharmacother.* **54**, 1001–1009 (2020).

30. Paik, J. Risdiplam: A Review in Spinal Muscular Atrophy. *CNS Drugs* **36**, 401–410 (2022).

31. Jablonka, S., Hennlein, L. & Sendtner, M. Therapy development for spinal muscular atrophy: perspectives for muscular dystrophies and neurodegenerative disorders. *Neurol. Res. Pract. 2021 41* **4**, 1–32 (2022).

32. Aslesh, T. & Yokota, T. Restoring SMN Expression: An Overview of the Therapeutic Developments for the Treatment of Spinal Muscular Atrophy. *Cells* **11**, (2022).

33. Vardatsikos, G., Sahu, A. & Srivastava, A. K. The insulin-like growth factor family: molecular mechanisms, redox regulation, and clinical implications. *Antioxid. Redox Signal.* **11**, 1165–1190 (2009).

34. Özdinler, P. H. & Macklis, J. D. IGF-I specifically enhances axon outgrowth of corticospinal motor neurons. *Nat. Neurosci. 2006 911* **9**, 1371–1381 (2006).

35. Brisson, B. K., Barton, E. R., Wang, Q. & Shewchuk, B. M. New modulators for IGF-I activity within IGF-I processing products. (2013). doi:10.3389/fendo.2013.00042

36. Delafontaine, P., Song, Y. H. & Li, Y. Expression, Regulation, and Function of IGF-1, IGF-1R, and IGF-1 Binding Proteins in Blood Vessels. *Arterioscler. Thromb. Vasc. Biol.*

24, 435–444 (2004).

37. Schiaffino, S. & Mammucari, C. *Regulation of skeletal muscle growth by the IGF1-Akt/PKB pathway: insights from genetic models*. (2011). doi:10.1186/2044-5040-1-4

38. Murdocca, M. *et al.* IPLEX Administration Improves Motor Neuron Survival and Ameliorates Motor Functions in a Severe Mouse Model of Spinal Muscular Atrophy. *Mol. Med.* **18**, 1076 (2012).

39. Hua, Y. *et al.* Peripheral SMN restoration is essential for long-term rescue of a severe SMA mouse model. *Nature* **478**, 123 (2011).

40. Yesbek Kaymaz, A. *et al.* Serum IGF1 and IGFBP3 levels in SMA patients. *Neuromuscul. Disord.* **26**, S105 (2016).

41. Brener, A. *et al.* Insulin-like growth factor-1 status is associated with insulin resistance in young patients with spinal muscular atrophy. *Neuromuscul. Disord.* **30**, 888–896 (2020).

42. Millino, C. *et al.* Different atrophy-hypertrophy transcription pathways in muscles affected by severe and mild spinal muscular atrophy. *BMC Med.* **7**, 1–9 (2009).

43. Tsai, L. K. *et al.* Systemic administration of a recombinant AAV1 vector encoding IGF-1 improves disease manifestations in SMA mice. *Mol. Ther.* **22**, 1450–1459 (2014).

44. Tsai, L. K. *et al.* IGF-1 delivery to CNS attenuates motor neuron cell death but does not improve motor function in type III SMA mice. *Neurobiol. Dis.* **45**, 272–279 (2012).

45. Bosch-Marcé, M. *et al.* Increased IGF-1 in muscle modulates the phenotype of severe SMA mice. *Hum. Mol. Genet.* **20**, 1844–1853 (2011).

46. Bosch-Marcé, M. *et al.* Increased IGF-1 in muscle modulates the phenotype of severe

SMA mice. *Hum. Mol. Genet.* **20**, 1844–1853 (2011).

47. Beyfuss, K. & Hood, D. A. Redox Report Communications in Free Radical Research A systematic review of p53 regulation of oxidative stress in skeletal muscle A systematic review of p53 regulation of oxidative stress in skeletal muscle. (2018). doi:10.1080/13510002.2017.1416773

48. Lakin, N. D. & Jackson, S. P. Regulation of p53 in response to DNA damage. *Oncogene 1999 1853* **18**, 7644–7655 (1999).

49. Williams, A. B. & Schumacher, B. p53 in the DNA-Damage-Repair Process. *Cold Spring Harb. Perspect. Med.* **6**, (2016).

50. Memme, J. M., Oliveira, A. N. & Hood, D. A. p53 regulates skeletal muscle mitophagy and mitochondrial quality control following denervation-induced muscle disuse. *J. Biol. Chem.* **298**, (2022).

51. Aubrey, B. J., Kelly, G. L., Janic, A., Herold, M. J. & Strasser, A. How does p53 induce apoptosis and how does this relate to p53-mediated tumour suppression? *Cell Death Differ. 2018 251* **25**, 104–113 (2017).

52. Young, P. J. *et al.* A Direct Interaction between the Survival Motor Neuron Protein and p53 and Its Relationship to Spinal Muscular Atrophy *. *J. Biol. Chem.* **277**, 2852–2859 (2002).

53. Simon, C. M. *et al.* Converging Mechanisms of p53 Activation Drive Motor Neuron Degeneration in Spinal Muscular Atrophy. *Cell Rep.* **21**, 3767–3780 (2017).

54. Courtney, N. L., Mole, A. J., Thomson, A. K. & Murray, L. M. Reduced P53 levels

ameliorate neuromuscular junction loss without affecting motor neuron pathology in a mouse model of spinal muscular atrophy. doi:10.1038/s41419-019-1727-6

55. Reedich, E. J., Kalski, M., Armijo, N., Cox, G. A. & DiDonato, C. J. Spinal motor neuron loss occurs through a p53-and-p21-independent mechanism in the Smn2B/− mouse model of spinal muscular atrophy. *Exp. Neurol.* **337**, 113587 (2021).

56. Eshraghi, M., McFall, E., Gibeault, S. & Kothary, R. Effect of genetic background on the phenotype of the Smn2B/- mouse model of spinal muscular atrophy. *Hum. Mol. Genet.* **25**, 4494–4506 (2016).

57. Puche, J. E. & Castilla-Cortázar, I. Human conditions of insulin-like growth factor-I (IGF-I) deficiency. (2012). doi:10.1186/1479-5876-10-224

58. Fayzullina, S. & Martin, L. J. Skeletal Muscle DNA Damage Precedes Spinal Motor Neuron DNA Damage in a Mouse Model of Spinal Muscular Atrophy (SMA). *PLoS One* **9**, (2014).

59. Memme, J. M., Oliveira, A. N. & Hood, D. A. p53 regulates skeletal muscle mitophagy and mitochondrial quality control following denervation-induced muscle disuse. *J. Biol. Chem.* **298**, 101540 (2022).